Spring 2010

Fabrication of a memory device using polyaniline nanofibers and gold nanoparticles

Krunal R. Waghela

Department:

FABRICATION OF A MEMORY DEVICE USING POLYANILINE NANOFIBERS AND GOLD NANOPARTICLES

by

KRUNAL R. WAGHELA

A THESIS

Presented to the Faculty of the Graduate School of the

MISSOURI UNIVERSITY OF SCIENCE AND TECHNOLOGY

In Partial Fulfillment of the Requirements for the Degree

MASTER OF SCIENCE IN CHEMICAL ENGINEERING

2010

Approved by

Jee-Ching Wang, Advisor
Frank D. Blum, Co-Advisor
Chang-Soo Kim

PUBLICATION THESIS OPTION

This thesis has been prepared in the styles utilized by the Advanced Materials journal. Section 3 (page 62-75) will be submitted for publication in the Advanced Materials journal.

ABSTRACT

Fabrication of a memory device using one-step/one-pot synthesis for making a PANI (polyaniline)/Au nanocomposite is reported. Although various devices with horizontal and vertical electrode structures were made, the basic structure used consisted of a PANI/Au thin film sandwiched between two electrodes. The ratio of the current in the OFF state to the current in the ON state was seen to be as high as 5000. These devices showed a bistable behavior, which is typical of memory devices. The PANI/Au nanocomposite thin film was constructed right on the electrode using microfabrication techniques with ultraviolet irradiation. The fabrication techniques discussed in this paper are highly scalable for mass production at an industrial scale and show that PANI/Au nanocomposite based memory devices can be readily manufactured by using traditional methods of microfabrication used for making semiconductive electronic memory devices.

ACKNOWLEDGMENTS

I would like to thank my advisor, Dr. Jee-Ching Wang, for his valuable guidance during my research. I would also like to thank my co-advisor, Dr. Frank Blum, for his support and guidance throughout this project to make it successful. His prudent advice has been extremely helpful and encouraging. I also appreciate the support received from Dr. Chang-Soo Kim who guided me at each and every step of this project. Special thanks, as well, to the members of Dr. Blum's and Dr. Kim's research groups for their encouragement and help. I appreciate the assistance of Dr. Scott Miller in the characterization of nanocomposite samples. A special thanks to Barbara Harris for proofreading my research work. I am grateful to the Department of Chemical Engineering and the Department of Chemistry at the Missouri University of Science and Technology and the National Science Foundation for providing the necessary financial assistance.

Above all, I would like to thank my mom and dad from the bottom of my heart for their love and support, and the encouragement that they have given me all my of life. I am really thankful to them for providing me with so many opportunities and for helping me succeed during the various phases of my life. I dedicate this thesis to my parents.

TABLE OF CONTENTS

LIST OF ILLUSTRATIONS

1. INTRODUCTION

1.1. CONDUCTIVE POLYMERS

In 1963, Weiss et al. showed that polypyrrole exhibits high conductivity when doped with iodine.[1,2,3] Scientists have focused on conductive polymers since the late 1970's after Hideshi Shirakawa, Alan G. MacDiarmid, Alan J. Heeger and their coworkers discovered that iodine-doped polyacetylene also showed high conductivity.[4,5] In short, doping can increase the conductivity of conjugated polymers. Polyaniline, polythiophene, polypyrrole and poly(dioctyl-bithiophene) are some of the examples of conjugated polymers that show this behavior. These rigid-backbone polymers and their mixed co-polymers, together, can be referred to as "melanins". Such a class of materials, with the mechanical properties of plastics and the conductive properties of metals or semiconductors, is referred to as "plastic electronics" or "organic semiconductors". Figure 1.1 shows structures of some common conductive polymers.

Conductive polymers differ in their backbone structure from nonconductive polymers. Polymers containing their valence electrons in sp^3 hybrid orbitals have strong covalent bonds which make these valence electrons less mobile as they are tightly bound in the valence band. For conjugated polymers like polyaniline, the backbone contains π bonds in p_z orbitals and sigma bonds in sp^2 hybrid orbitals. Pi bonds are much weaker than sigma bonds and, thus, valence electrons are more loosely bound making them more mobile. Some of these valence electrons can also be removed when doped with an electron acceptor. This type of doping results in oxidation and is called p-type doping. When doped with an electron donor, more loosely bound electrons are produced resulting

in reduction. This type of doping is called n-type doping. However, p-type doping is a method that is preferred and is more commonly used than the n-type method because polymers containing n-type dopants are usually unstable in air as they can be oxidized by atmospheric oxygen.[6]

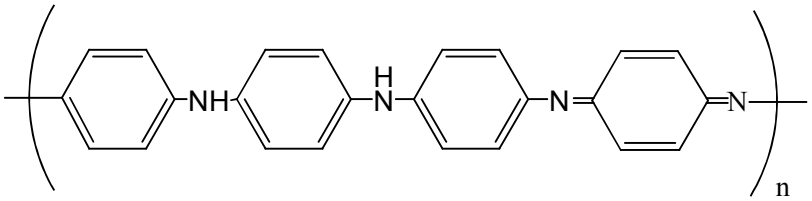

Polyaniline (Emeraldine form), (PANI)

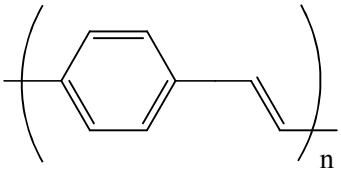

Poly(p-phenylene vinylene), (PPV)

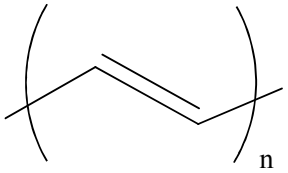

Polyacetylene, (PA)

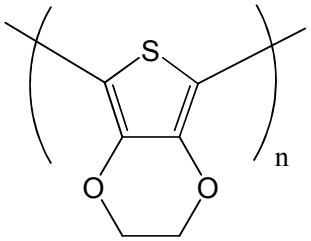

Poly(3,4-ethylenedioxythiophene), (PEDOT)

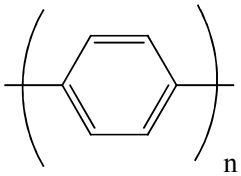

Poly(p-phenylene), (PPP)

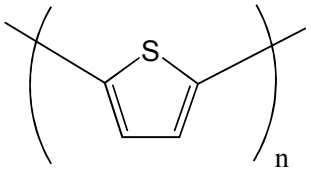

Polythiophene, (PTh)

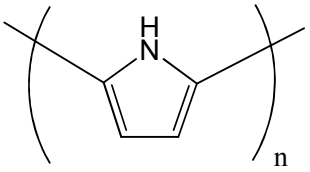

Polypyrrole, (PPy)

Figure 1.1. Structures of some common conductive polymers.

The process of doping a conjugated polymer results in the formation of a band of p-orbitals, where the electrons have higher mobility due to unbalanced electron-hole pairs. As a result, conductivity of conjugated polymers can be greatly increased by doping. The level of doping controls the unbalanced number of electron-hole pairs (charge carriers) and, thereby, controls the conductivity.[7] The conductivity of polyaniline has been reported to change from 10^{-10} S/cm (intrinsic state) to 10^{2} S/cm (doped state).[8] Methods like charge injection doping, chemical doping, electrochemical doping, photo doping, etc., can also be used to dope conjugated polymers. Doping results in charge transfer between the dopant and the polymer. The level of doping is affected by the distribution and the type of dopant used in the process.[7-16] A p-type doping process results in the formation of polarons (a fermionic quasiparticle composed of a charge and its electric polarization field) which may be followed by the formation of bipolarons (part of a macromolecular system containing two positive charges in a conjugated system) in the second step. This mechanism is represented in Figure 1.2.

$$\mathbf{P_n \rightleftharpoons P_n^{+} + e^{-}}$$

$$\mathbf{P_n^{+} \rightleftharpoons P_n^{2+} + e^{-}}$$

Figure 1.2. Polaron and bipolaron formation mechanism.

Conductive polymers have a wide variety of uses, especially in microelectronics, as their mechanical properties are superior to those of traditional semiconductors. They can be used in photogalvanic cells, light emitting diodes, gas sensors, memory devices,

actuators, etc.[17-20] Consequently, scientists have a strong interest in conductive polymers that might replace traditional semiconductors in many applications, as stated above.

1.2. POLYANILINE

Polyaniline (PANI) has been of interest to a large number of researchers because of its important properties like: wide range of conductivity, ease of synthesis, low cost of aniline, stability in ambient atmosphere and reversible doping/de-doping ability.[21] Polyaniline is formed by oxidative polymerization of aniline. Various methods (such as chemical oxidation, electrochemical oxidation, etc.) have been developed to oxidize aniline to form PANI.[22-26] Aniline can be chemically oxidized in the presence of an acid dopant with a strong oxidizing agent such as ammonium persulfate.[22,23] The mechanism of this oxidative polymerization of aniline is not completely understood, although multiple paths have been suggested for it.

A widely accepted mechanism describes the formation of anilinium cation-radical during the polymerization process, as seen in Figure 1.3.[27-30] The first step is oxidizing aniline using an oxidizing agent which leads to the formation of an anilinium cation-radical. Two cation-radicals can combine to form a dimer, called N-phenyl-1,4-phenylenediamine (p-aminophenylamine), in the presence of an acid. The dimer can react with a monomer to form a trimer which gets readily oxidized and can combine with another monomer to form a tetramer. Two dimers can also react to form a tetramer. Finally, the chain keeps increasing in length to form a polymer. Oxidants, such a ammonium persulphate, hydrogen peroxide, benzoyl peroxide, and choloroauric acid can be used to oxidize aniline.

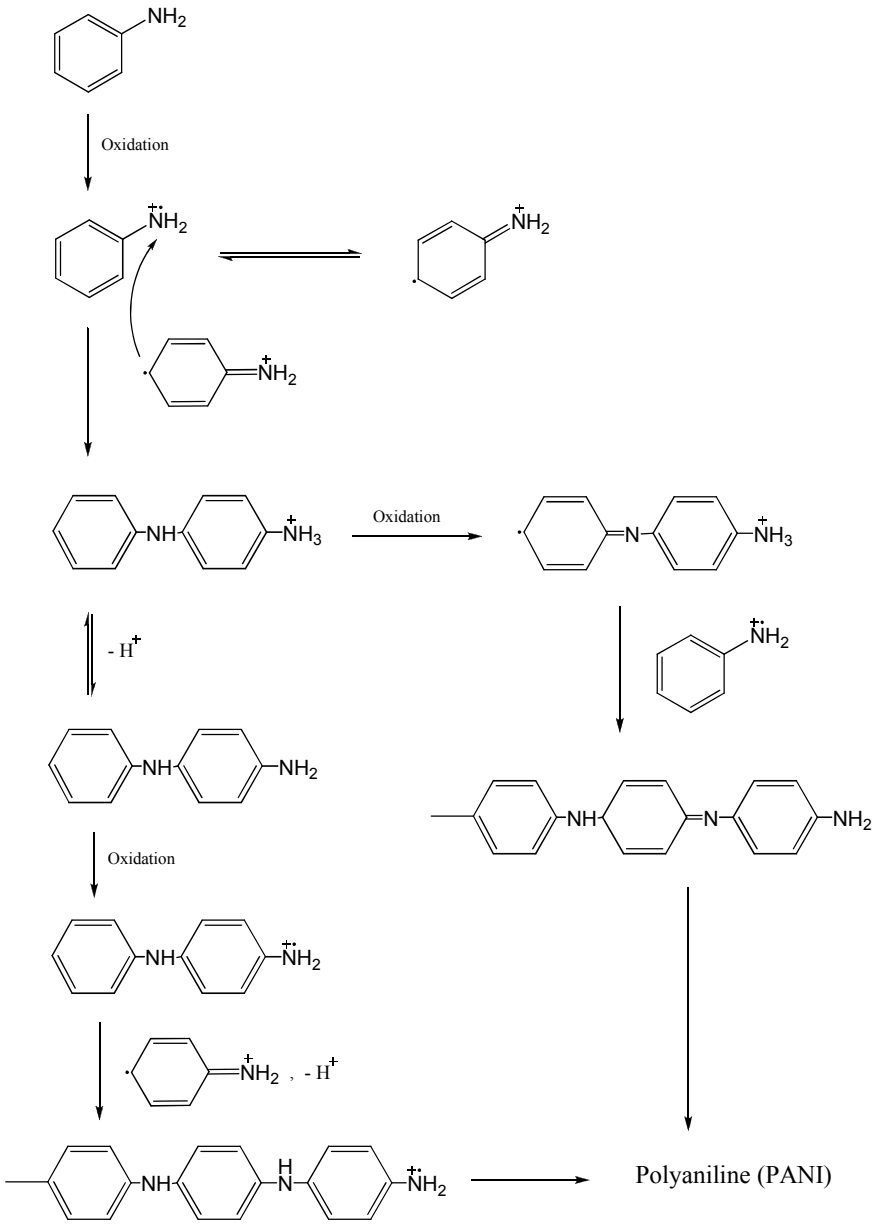

Figure 1.3. Polymerization mechanism of Aniline.

PANI exists in a variety of oxidized states such as leucoemeraldine (fully reduced), pernigraniline (fully oxidized), emeraldine (semi-oxidized), protomeraldine and nigraniline, which can be seen in Figure 1.4.[31] Emeraldine is of most interest as its doped form is highly conductive and stable in the atmosphere.[31] Neither pernigraniline

(completely intrinsically oxidized) nor leucoemaraldine are conductive and, therefore, are not of great interest. Emeraldine is generally doped with a protic acid by the method called protic acid doping to form highly conductive PANI, as seen in Figure 1.5.

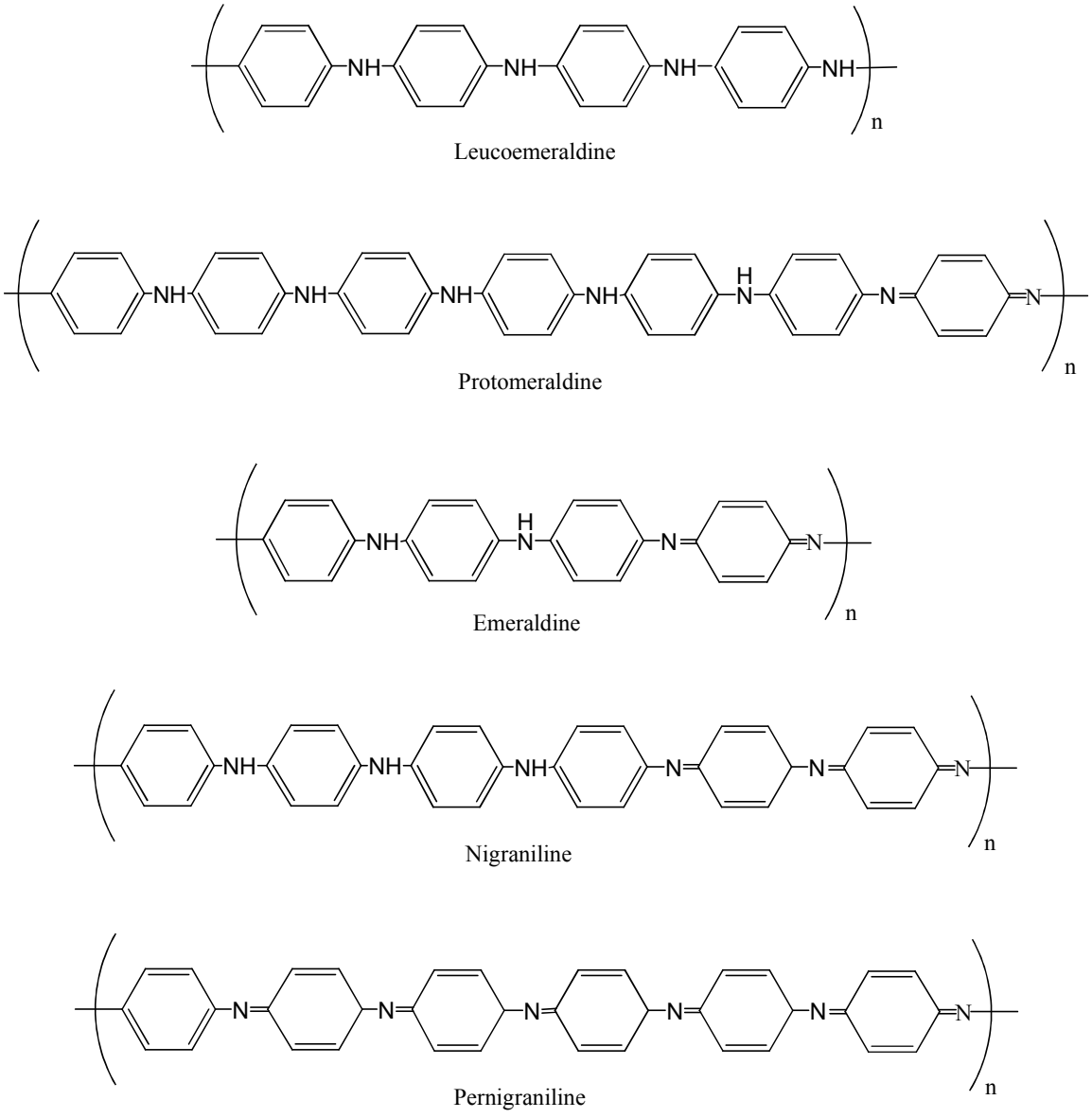

Figure 1.4. Different oxidized states of PANI.

Leucoemeraldine looks white or clear, whereas emeraldine looks blue/green and pernigraniline looks green/violet. This difference can be used as a primitive basic visual test to distinguish between various oxidized states of PANI.

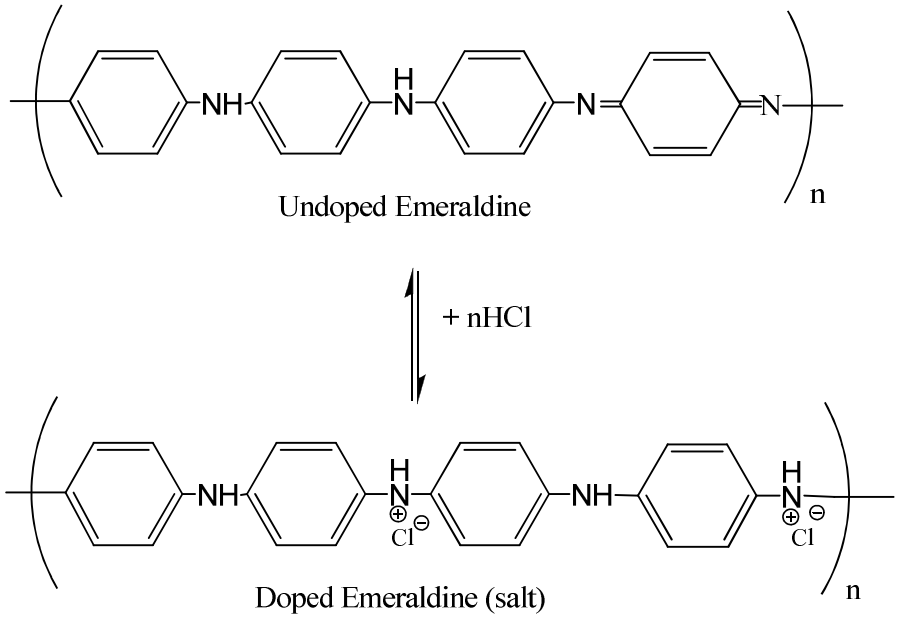

Figure 1.5. Protonic acid doping of PANI.

Though PANI has interesting conductive properties, its use has been limited due to its poor solubility in common solvents and its problematic processability. Scientists have tried to tackle this problem by increasing its solubility, making co-polymers of PANI, introducing organically soluble groups in the polymer backbone, making water soluble PANI, dispersion polymerization, pH-controlled PANI colloids, etc.[32-35] However, many methods lead to reduced conductivities and, hence, are not very useful. Also, certain applications require the formation of uniform thin films of PANI for

semiconductive applications, such as in MEMS devices, photovoltaic cells and memory devices. One such method uses electrostatic interactions and H-bonding to create multiple layers, one on another, to form thin films.[36] The processability of PANI has been improved, with the help of these methods, but further research is still required to develop viable processes for mass production and industrial use.

1.3. POLYANILINE NANOSTRUCTURES AND NANOCOMPOSITES

It is well known that nanostructures have much larger specific surface areas than those of similar bulk substances with the same volume. For conductive polymers, an increase in the surface area leads to an increase in sensitivity. Thus, polymeric nanostructures are of great importance because of their superior conductive properties for semiconductive devices. Nanostructures of PANI have been made in various shapes like nanorods, nanofibers, nanowires, nanotubes, etc., and have been shown to have significantly better sensing and catalytic properties than those of bulk PANI.[37-40]

Various methods have been used to develop nanostructures of conductive PANI, including physical, as well as chemical methods, that involved electrospinning, mechanical stretching, porous alumina and polycarbonate templates, surfactants, micelles, etc.[41-48] Recently, methods like interfacial polymerization and nanofiber seeding, have been developed as a template-less syntheses.[49-50] Our research group has gone even further and developed a one-step process that produces conductive PANI nanofibers by using gamma rays and UV radiation.[51-54]

To incorporate the use of PANI nanostructures in semiconductive operations, methods like photolithography, e-beam lithography, laser writing and dip pen lithography have proved to be useful.[55-58] These methods are traditionally used for patterning

semiconductive and MEMS devices and it is very advantageous now that these methods have proved to be useful for patterning pattern PANI nanostructures as well.

To improve certain properties of conductive polymer nanostructures, scientists have developed nanocomposite recipes that normally require the addition of inorganic nanostructures to these organic polymers. Properties of these nanocomposites have been improved more than those of organic conductive nanostructures. Nevertheless, some nanocomposite structures may have improved conductivity, whereas, others may have improved stability in certain environments. Some nanocomposites may also help a conductive polymer to exhibit properties that it may not normally have. This effect has also been shown for PANI nanocomposites.[59]

To improve the stability of polyaniline colloids, silica has been used to form a nanocomposite.[35,59] Nanoparticles of conductive metals, like Au, Ag, Pd, Pt, carbon nanotubes, etc., can be used to enhance the conductive properties of PANI nanofibers.[60-62] Noble metal nanoparticles are used as they are resistant to the majority of harsh chemical environments. Thus, improvements in properties of these materials make them appropriate for use in non-volatile memory devices, sensors, photovoltaic cells, etc. The manner of the attachment, interface and dispersion of these inorganic nanoparticles in the polymer matrix plays a key role in determining the combined properties of a nanocomposite.[63-64]

1.4. POLYANILINE NANOCOMPOSITE BASED MEMORY DEVICES

Organic conducting polymers are much less expensive than traditional semiconductors. They also possess flexibility that can be used to build thin film electronic devices on flexible substrates.[65,66] Various researchers have shown that organic

conducting polymers can be used for making some of the electronic devices like light emitting diodes,[67,68] various memory devices, [60,69-75] solar cells [76-78] and transistors.[79-81]

Researchers have used various conjugated polymer nanostructures, decorated with other inorganic nanoparticles, to produce memory devices.[82] Because polyaniline shows strong potential for the same use, many researchers have tried to develop memory devices using polyaniline nanocomposites.[60,83-84]

A typical PANI/Au nanocomposite memory device is represented in Figure 1.6. As seen in the figure, an electrode layer is prepared on top of the substrate. A PANI/Au nanocomposite layer is then formed on the bottom electrode. Next, a top electrode is formed or brought in contact with an active memory layer made up of the PANI/Au nanocomposite. Once the assembly is complete, a potential difference is applied between the two electrodes. It does not matter which electrode is connected to the positive or the negative terminal of the electrometer.

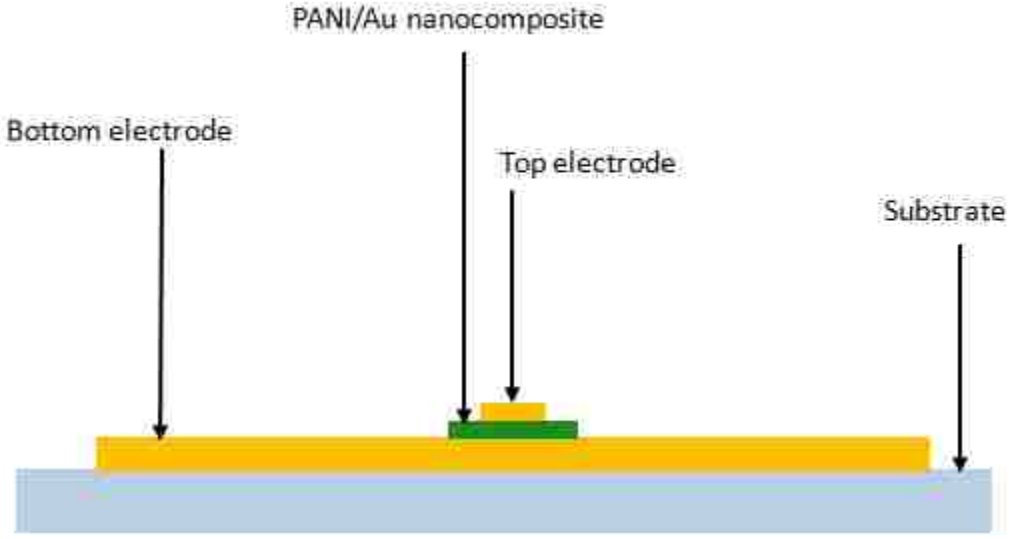

Figure 1.6. A typical PANI/Au nanocomposite memory device.

To test the device and determine if it exhibits memory characteristics, a voltage scan of 0 to around 5 to 6 volts can be used. Many semiconductor integrated circuits and memory devices have a working voltage of around 5 volts and, hence, it is important that a PANI/Au memory device function in the same range. If the device does not appropriately function in this range, then factors which affect its performance need to be adjusted. In general, a memory device shows a characteristic transition voltage. This is the switching voltage at which the device can be turned from the OFF state to the ON state, and vice versa. The OFF state of a device is represented by low current characteristics and continues up to the transition voltage. When the voltage is greater than the transition voltage, the current shows an abrupt increase, which may be several orders of magnitude. Figure 1.7 represents typical memory device characteristics. The current stays in this higher range after the transition voltage, and increases with an increase in voltage, except for the negative differential resistance (NDR) region.[60]

Some memory devices possess a negative differential resistance region in the ON state which is defined by a relatively small decrease in the current with an increase in voltage that is attributed to a rapid recombination of charges in random directions. This rapid recombination of charges creates a cancelling effect that leads to a decrease in the current. However, the current still remains within the higher magnitude range, even though the current decreases slightly in this region.

A device can be turned from the OFF state to the ON state by a pulse of any voltage greater than the transition voltage. Also, the device can be turned OFF from the ON state by a pulse of a negative voltage, which may have an absolute value that is higher than the transition voltage. For a device to be a non-volatile memory device, it

should retain its OFF state or ON state, for an infinite time ideally, after the voltage source is removed. In other words, if the transition voltage is +2.5 V and a pulse of +4 V is applied to the device, it turns to the ON state. Once the voltage source is disconnected, it should retain its ON state. A reading voltage of around +1.2 volts, for example, should generate a current of higher magnitude that corresponds to the ON state characteristics. If a voltage pulse of -5 V is applied to the device, the state changes to the OFF state. At a reading voltage of +1.2 V, the device should generate a current that corresponds to the lower magnitude (corresponding to the OFF state). Such a device can be termed as a non-volatile read-write memory device.

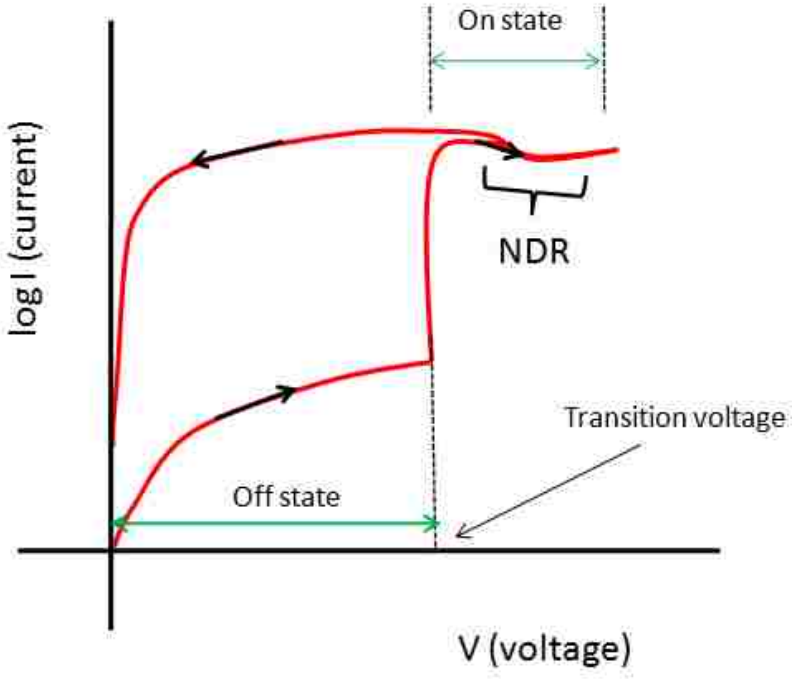

Figure 1.7. Characteristics of a typical memory device.

Some of the PANI/Au memory devices can operate only under high vacuum.[60] Also, most of these devices require multiple steps in their production, making it difficult to achieve a viable process that is fast enough for commercial manufacturing.

The purpose of this research is to develop an inexpensive one-step method to easily produce a polyaniline/Au nanocomposite memory device that can function satisfactorily in normal environmental conditions. Section 2 describes some fabrication methods and characterization of a PANI/Au nanocomposite memory device.

1.5. REFERENCES

1. McNeill, R.; Siudak, R.; Wardlaw J. H.; Weiss D. E. *Aust. J. Chem.* **1963**, 16, 1056.
2. Bolto, B. A.; Weiss, D. E. *Aust. J. Chem.* **1963**, 16, 1076.
3. McNeill, R.; Bolto, B. A.; Weiss, D. E. *Aust. J. Chem.* **1963**, 16, 1090.
4. Shirakawa, H.; Louis, E. J.; MacDiarmid, A. G.; Chiang, C. K.; Heeger, A. J. *Chem. Commun.* **1977**, 578.
5. Chiang, C. K.; Fincher, C. R.; Park, Y. W.; Heeger, A. J.; Shirakawa, H.; Louis, E. J.; Gau, S. C.; MacDiarmid, A. G. *Phys. Rev. Lett.* **1977**, 39, 1098.
6. De Leeuw, D.M.; Simenon, M.M.J.; Brown, A.R.; Einerhand, R.E.F. *Synth. Met.* **1997,** 87, 53.
7. Onodera, Y. *Phys. Rev. B* **1984**, 30, 775.
8. Yu, L. T.; Borredon, M. S.; Jozefowicz, M.; Belorgey, G.; Buvet, R. *J. Polym. Sci.* ***1987,*** 10*, 2931*.
9. Heeger, A. J.; Kivelson, S.; Schrieffer, J. R.; Su, W. P. *Rev. Mod. Phys.* **1988**, 60, 781.
10. Bredas, J. L.; Beljonne, D.; Coropceanu, V.; Cornil, J. *Chem. Rev*. **2004**, 104, 4971.
11. Chiang, C. K.; Gau, S. C.; Fincher, C. R.; Park, Y. W.; MacDiarmid, A. G.; Heeger, A. J. *Appl. Phys. Lett.* **1978**, 33, 18.

12. Francois, B.; Bernard, M.; Andre, J. J. *J. Chem. Phys.*, **1985**, 75, 4142.

13. Nigrey, P. J.; MacDiarmid, A. G.; Heeger, A. J. *J Chem. Soc, Chem. Comm.* **1979**, 594.

14. Nigrey, P. J.; MacInnes, D. Jr.; Nairns, D. P.; MacDiarmid, A. G.; Heeger, A. J. *J. Electrochem. Soc.* **1981**, 128, 1651.

15. MacInnes, D. Jr.; Druy, M. A.; Nigrey, A. J.; Nairns, D. P.; MacDiarmid, A. G.; Heeger, A. J. *J. Chem. Soc., Chem. Commun.* **1981**, 317.

16. Diaz, A. F.; Clarke, T. C. *J . Electroanal. Chem.* **1980**, 111, 115.

17. Chen, S. N.; Heeger, A. J.; Kiss, Z.; MacDiarmid, A. G.; Gau, S. C.; Peebles, D. L. *Appl. Phys. Lett.* **1980**, 36, 96.

18. Burroughes, J. H.; Bradley, D. D. C.; Brown, A. R.; Marks, R. N.; Friend, R. H.; Burn, P. L.; Holmes, A. B. *Nature* **1990**, *347*, 539.

19. Nylander, C.; Armgarth, M.; Lundstrm, I. *Anal. Chem. Symp. Ser*. **1983**, 17, 203.

20. Tseng, R. J.; Huang, J.; Ouyang, J.; Kaner, R. B.; Yang, Y. *Nano. Lett*. **2005**, 5, 1077.

21. Kang, E. T.; Neoh, K. G.; Tan, K. L. *Prog. Polym. Sci.* **1998**, *23*, 211.

22. Scherr, E. M.; MacDiarmid, A. G.; Manohar, S. K.; Masters, J. G.; Sun, Y.; Tang, X.; Druy, M. A.; Glatkowski, P. J.; Cajipe, V. B.; Fischer, J. E.; Cromack, K. R.; Jozefowitcz, M. E.; Ginder, J. M.; McCall, R. P.; Epstein, A. J. *Synth. Met.* **1991**, 41, 735.

23. Epstein, A. J.; Ginder, J. M.; Zuo, F.; Bigelow, R. W.; Tanner, D. B.; Richter, A. F.; Huang, W. S.; MacDiarmid, A. G. *Synth. Met.* **1987**, 18, 303.

24. Mohilner, D. M.; Adams, R. H.; Argersinger Jr, W. J. *J. Am. Chem. Soc,* **1962**, 84, 3618.

25. Diaz, A. F.; Logan, *J. A. J. Electroanal. Chem.* **1980**, 111, 111.

26. Wang, B.; Tang, J.; Wang, F. *Synth. Met.* **1986**, 13, 329.

27. Wei, Y.; Tang, X.; Sun, Y.; Focke, W. *J Polym Sci, Polym Chem Ed* **1989**, *27*, 2385.

28. Stejskal, J.; Kratochvil, P.; Spirkova, M. *Polymer* **1995**, *36*, 4135.

29. Neudeck, A.; Petr, A.; Dunsch, L. *Synth. Met.*, **1999**, 107, 143.

30. Bodalia, R. R.; Duran, R. S. *J. Am. Chem. Soc.* **1993**, *115*, 11467.

31. Pandey, S. S.; Annapoorni, S.; Malhotra, B. D. *Macromolecules* **1993**, 26, 3190.

32. Bereeron. J. Y.; Dao. L. H. *Macromolecules* **1992**, 25, 3332.

33. Kinlen, P. J.; Liu, J.; Ding, Y.; Graham, C. R.; Remsen, E. E *Macromolecules* **1998**, 31*,* 1735.

34. Chen, S-A.; Hwang, G-W.; *J. Am. Chem. Soc.* **1995**,117, 10055.

35. Stejskal, J.; Sapurina, I. *J. Colloid Interface Sci.* **2004**, *274*, 489.

36. Stockton, W. B.; Rubner, M. F. *Macromolecules* **1997**, *30*, 2717.

37. Virji, S.; Huang, J.; Kaner, R. B.; Weiller, B. H. *Nano Lett.* **2004**, *4*, 491.

38. Liu, H.; Kameoka, J.; Czaplewski, D. A.; Craighead, H. G. *Nano Lett.* **2004,** 4, 6715.

39. Kanungo, M.; Kumar, A.; Contractor, A. Q. *Anal. Chem.* **2003**, *75*, 5673.

40. Janata, J.; Josowicz, M. *Nat. Mater.* **2003**, *2*, 19.

41. Reneker, D. H.; Chun, I. *Nanotechnology* **1996**, *7*, 216-223.

42. MacDiarmid, A. G.; Jones, W. E.; Norris, I. D.; Gao, J.; Johnson, A. T.; Pinto, N. J.; Hone, J.; Han, B.; Ko, F. K.; Okuzaki, H.; Llaguno, M. *Synth. Met.* **2001**, *119*, 27.

43. He, H. X.; Li, C. Z.; Tao, N. J. *Appl. Phys. Lett.* **2001**, *78*, 811.

44. Wang, C. W.; Wang, Z.; Li, M. K.; Li, H. L. *Chem. Phys. Lett.* **2001**, *341*, 431.

45. Martin, C. R. *Chem. Mater.* **1996**, *8*, 1739.

46. Parthasarathy, R. V.; Martin, C. R. *Chem. Mater.* **1994**, *6*, 1627.

47. Michaelson, J. C.; McEvoy, A. J. *Chem. Commun.* **1994**, 79.

48. Qiu, H. J.; Wan, M. X. *J. Polym. Sci., Part A: Polym. Chem.* **2001**, *39*, 3485.

49. Huang, J. X.; Virji, S.; Weiller, B. H.; Kaner, R. B. *J. Am. Chem Soc.* **2003**, *125*, 314.

50. Zhang, X. Y.; Goux, W. J.; Manohar, S. K. *J. Am. Chem. Soc.* **2004**, *126*, 4502.

51. Pillalamarri, S. K.; Blum, F. D.; Tokuhiro, A. F.; Story, J. G.; Bertino, M. F. *Chem. Mater.* **2005**, 17, 227.

52. Werake, L.K.; Story, J.G.; Bertino, M.F.; Pillalamarri, S.K.; Blum, F.D. *Nanotech.* **2005**, 16, 2833.

53. Blum, F. D.; Li, Z.; S. K. Pillalamarri, S. K.; Bertino, M. F. *Polymer Preprints*, **2007**, 48, 55.

54. Blum, F. D.; Pillalamarri, S.K.; Werake, L. K.; Story, J. G.; Bertino, M. F.; Tokuhiro, A. K. *Polymer Preprints* **2006**, 47, 405.

55. Gorman, C. B.; Biebuyck, H. A.; Whitesides, G. M. *Chem. Mater*. **1995**, 7, 526.

56. Garnier, F.; Hadjlaoui, R.; Yasser, A. Scivastava, P. *Science* **1994,** 265, 1684.

57. Bargon, J.; Behnck, W.; Weidenbrueck, T.; Ueno, T. *Synth. Met*. **1991**, 41, 1111.

58. Maynor, B. W.; Filocamo, S. F.; Grinstaff, M. W.; Liu, J. J. *Am. Chem. Soc*. **2002**, 124, 522.

59. Gangopadhyay, R.; De, A. *Chem. Mater.* **2000**, *12*, 608.

60. Tseng, R. J.; Huang, J. X.; Ouyang, J.; Kaner, R. B.; Yang, Y. *Nano Lett*. **2005**, 5 1077.

61. Pillalamarri, S.K.; Blum, F.D.; Tokuhiro, A.T.; Story, J.G.; Bertino, M.F. *Chem. Mater.* **2005**, 17, 5941.

62. Ali, S. R.; Ma, Y.; Parajuli, R. R.; Balogun, Y.; Lai, L. W.; He, H. *Anal. Chem.* **2007**, 79, 2583.

63. Fahlman, M.; Salaneck, W.R. *Surf. Sci*. **2002**, 500, 904.

64. Advincula, R. C. *J. Dispersion Sci. Technol*. **2003**, 24, 343.

65. Baldo, M. A.; O'Brien, D. F.; You, Y., Shoustikov, A.; Sibley, S.; Thompson, M. E.; Forrest, S. R. *Nature* **1998**, 395, 151.

66. Heringdorf, F.; Reuter, M. C.; Tromp, R. M. *Nature* **2001**, 412, 517.

67. Friend, R. H.; Gymer, R. W.; Holmes, A. B.; Burroughes, J. H.; Marks, R. N.; Taliani, C.; Bradley, D. D. C.; Dos Santos, D. A.; Bre´das, J. L.; Lögdlund, M.; Salaneck, W. R. *Nature* **1999**, 397, 121.

68. Müller, C. D.; Falcou, A.; Reckefuss, N.; Rojahn, M.; Wiederhirn, V.; Rudati, P.; Frohne, H.; Nuyken, O.; Becher, H.; Meerholz, K. *Nature* **2003**, 421, 829.

69. Scott, J. C. *Science* **2004**, 304, 62.

70. Chen, Y.; Ohlberg, D. A. A.; Li, X.; Stewart, D. R.; Williams, R. S.; Jeppesen, J. O.; Nielsen, K. A.; Stoddart, J. F.; Olynick, D. L.; Anderson, E. *Appl. Phys. Lett*. **2003**, 82, 1610.

71. Ma, L. P.; Liu, J.; Yang, Y. *Appl. Phys. Lett*. **2002**, 80, 2997.

72. Ma, L. P.; Pyo, S.; Ouyang, J.; Xu, Q. F.; Yang, Y. *Appl. Phys. Lett*. **2003**, 82, 1419.

73. Bozano, L. D.; Kean, B. W.; Deline, V. R.; Salem, J. R.; Scott, J. C. *Appl. Phys. Lett*. **2004**, 84, 607.

74. Ouyang, J.; Chu, C. W.; Szmanda, C. R.; Ma, L. P.; Yang, Y. *Nat. Mater*. **2004**, 3, 918.

75. Wu, J.; Ma, L. P.; Yang, Y. *Phys. Rev. B* **2004**, 69, 115321.

76. Yu, G.; Gao, J.; Hummelen, J. C.; Wudl, F.; Heeger A. J. *Science* **1995**, 270, 1789.

77. Brabec, C. J.; Sariciftci, N. S.; Hummelen, J. C. *Adv. Funct. Mater*. **2001**, 11, 15.

78. Sariciftci, N. S.; Smilowitz, L.; Heeger, A. J.; Wudl, F. *Science* **1992**, 258, 1474.

79. Ma, L; Yang, Y. *Appl. Phys. Lett*. **2004**, 85, 5084.

80. Sirringhuas, H.; Tessler, N.; Friend, R. H. *Science* **1998**, 280, 1741.

81. Dimitrakopoulos, C. D.; Mascaro, D. J. *IBM J. Res. Dev*. **2001**, 45, 11.

82. Yang, Y.; Ouyang, J.; Ma, L.; Tseng, R. J.; Chu, C. *Adv. Funct. Mater*. **2006**, 16, 1001.

83. Li, L.; Ling, Q. D.; Zhu, C.; Chan, D. S. H.; Kang, E. T.; Neoha K. G. *J. Elect. Soc*. **2008**, 155, H205.

84. Wei, D.; Baral, J. K.; Österbacka, R.; Ivaska, A. *J. Mat. Chem*. **2008**, 18, 53.

2. ONE-POT SYNTHESIS OF MEMORY DEVICES USING POLYANILINE AND GOLD NANOCOMPOSITES USING VARIOUS FABRICATION METHODS

2.1. INTRODUCTION

Electrically conductive polymers have opened up a new horizon because their properties can be superior to traditional semiconductors.[1,2] Thus, these conjugated polymers may possibly replace traditional semiconductors in a number of electronic devices. Scientists have already shown that conducting polymers can be used to make devices like solar cells,[3-5] sensors,[6-10] actuators,[11-12] memory devices,[13-22] light emitting diodes,[23-24] and transistors[25-27].

Polyaniline is one of several conductive polymers that have been studied extensively. Several researchers have attempted to make memory devices using polyaniline.[13-15] However, because a large number of steps are required in these procedures to fabricate the devices,[13-15] an extremely long time is consumed using these processes to produce multiple devices. Processes that can be scaled up for mass production and that require significantly fewer steps (and thus less time) are desirable for industrial and commercial applications.

Our group has already shown that microfabrication techniques can be used to make thin films of PANI nanofibers and nanocomposites using one-step/one-pot synthesis through UV irradiation.[10,28] These thin films are extremely suitable for semiconductive applications. This section describes various techniques that can be used to fabricate a memory device using one-step/one-pot synthesis with the application of UV irradiation. Synthesis of PANI/Au nanocomposites can be done right on the electrode

assembly and the device can be ready to use soon after polymerization. These devices were tested to determine their characteristics relative to a memory device. Thus, microfabrication techniques were used to produce PANI/Au nanocomposite-based memory devices using a superior fabrication technique that would be useful for fast commercial and industrial mass production.

2.2. EXPERIMENTAL

The overall device fabrication consists of fabricating the electrodes, followed by PANI/Au nanocomposite thin film synthesis.

2.2.1. Materials. Aniline and $HAuCl_4 \bullet 3H_2O$ were obtained from Alfa Aesar, and HCl and ammonium persulfate were obtained from Fisher Scientific. All chemicals were used as received, except aniline, which was distilled before use. Polydimethylsiloxance (PDMS), which was used as the substrate for making vertical devices from glass slides, was obtained from Dow Corning in a two-piece kit of Sylgard® 184 silicone elastomer base and curing agent. 75 mm x 25 mm x 1 mm plain precleaned micro glass slides were obtained from Dow Corning and 75 mm x 50 mm x 1 mm plain precleaned micro glass slides were obtained from Fisher Scientific. Su-8 2050 (negative photoresist) was obtained from MicroChem. S1818 (positive photoresist) and positive photoresist developer (MF™ CD-26) were obtained from ROHM & HAAS Electronic Materials. A positive photoresist stripper (Dyanostrip 7000) was obtained from Dynaloy. Dry film MX5050 was obtained from DuPont. Dry film developer (D-4000) was obtained from RBP Chemical Technologies. 4-inch (100 mm) mechanical grade silicon wafers (single side polished, <100>, 310-325 μm thickness) were obtained from University Wafer. Acetone and methanol (histological grade), for washing silicon wafers, were obtained

from Fisher Scientific. GE CA (cellulose acetate, diameter (ϕ) = 90 mm, pore size = 0.22 μm, thickness = 65 to 110 μm) and GE PETE (polyester, diameter (ϕ) = 90 mm, pore size = 10 μm, thickness = 6 to 11 μm) filter membranes were obtained from Pargreen Process Technologies.

2.2.2. Polyaniline Nanofibers and Polyaniline/Gold Nanocomposite Synthesis. Polyaniline nanofibers were prepared by one step synthesis. A total of 10 ml of deionized (DI) water, 0.1 M aniline, 0.3 M HCl and 0.05 M ammonium persulfate was mixed in a vial. 5 ml of DI water were placed in a vial with 97 μL aniline and 333 μL of 10.1 N (37 %) HCl. Another vial was filled with 5 ml of DI water and 0.0456 g ammonium persulfate. After addition of all of the reactants, the precursor solution was coated on the electrode and exposed to UV (365 nm – 5.4 mW/cm^2, 405 nm – 13 mW/cm^2, Cobilt CA-800 UV mask aligner) for 6 min. After UV exposure, the sample was dried under constant air flow for 4 to 5 h. After drying, the sample was washed with DI water and acetone to remove unreacted chemicals and then dried under constant air flow for about 12 h. Polyaniline nanofibers were prepared to compare results with PANI/Au nanocomposites.

Polyaniline/Au nanocomposites were also prepared using a similar one step synthesis. Typically, samples were prepared by placing 10 ml of DI water, 94 μL aniline (0.1 M), 0.3 M HCl and $HAuCl_4 \bullet 3H_2O$ in a vial. Various concentrations of $HAuCl_4 \bullet 3H_2O$ were used for different samples. Contents of one vial containing 5 ml of DI water, aniline and HCl were added to 5 ml of DI water and chloroauric acid in another vial. $HAuCl_4$, which acted as the oxidant for aniline, was reduced to form Au nanoparticles. Thus, the addition of chloroauric acid started the polymerization reaction. The solution was quickly

coated on the electrode for the horizontal device and was exposed to UV for 6 min. This precursor solution was also injected in the micro-channel for the vertical device and was exposed to UV for 6 min. Also, various samples were prepared using UV with an exposure time of 6, 13 and 20 min, for nanofiber characterization using a scanning electron microscope. The samples were dried under a constant air flow for about 4 to 5 h. After drying, the samples were washed with acetone and DI water to remove the unreacted chemicals, and again put under constant air flow for 12 h before being tested. The samples were ready for testing after this 12 hour drying.

2.2.3. Characterization. All the PANI/Au devices were characterized for their memory-like behavior by applying a voltage scan while measuring the current. Characterization of the memory device was done using a Keithley 617 programmable electrometer and a Keithley 4200SCS semiconductor parameter characterization system. The polarity of the electrodes is not of importance for measuring the memory characteristics in these devices. In other words, the leads to the device can be interchanged, i.e. the polarity can be switched between the electrodes. A sweep rate of 0.2 V/s was used to make characterization measurements using a Keithley 4200 semiconductor parameter analyzer. All experiments to measure the current characteristics of the memory devices were conducted at room temperature and atmospheric pressure.

Morphology of PANI and PANI/Au nanocomposites was characterized using Hitachi S-4700 Scanning Electron Microscope (SEM). The characterization was done at low accelerating voltage of 5 kV to avoid damage to the nanofibers that could occur at higher voltages. A high accelerating voltage may cause local heating and charging of the fibers and could damage their morphology. The images were obtained without tilt to

avoid projection distortion. A working distance of around 13 mm was used to image the bulk samples. For imaging the samples exposed to UV, a working distance of around 4 mm was used with an ultra-high resolution mode. A spot size of 6 on this electron microscope was used for low working distances to obtain sharper images. The stage was locked while obtaining images at very high magnification to avoid vibrations and blurring of the images. Only the upper detector was used to image the samples. At short working distances, there is hardly any signal at the lower detector and, hence, the use of a mixed detector was avoided as it would have made the images dark.

The thickness and thermal stability were monitored for some of the devices. The thickness of the various PANI/Au samples on the devices was measured, using a Tencor Alpha-Step 200 and thermogravimetric analysis (TGA) was used to determine the PANI to Au ratio in the sample. TGA measurements were made with air flowing at 100 cc/min and a ramp rate of 20 °C/min with a Hi-Res TGA 2950 Thermogravimetric analyzer (TA instruments). Contact angle measurements were made using a RAME-HART A-100 NRL Contact Angle Goniometer.

2.2.4. Horizontal Device Fabrication. A variety of designs of horizontal devices were made in order to test the suitability of the materials. Microfabrication and photolithography were used to fabricate many of these devices.

The fabrication procedure used for various horizontal devices is described in parts of Section 2.2.4, whereas, the details about the working and the problems with these devices are discussed in the results and discussion section (Section 2.3).

2.2.4.1 Horizontal device #1. This device was fabricated on a 4-inch Si wafer. The 4-inch silicon wafer was washed in acetone, methanol and then DI water, for 3 min

in each, to clean off surface impurities. The wafer was spin dried and then heated at 150 °C for 6 min to dry the sample. This silicon wafer was used as the substrate for the device. Next, a 50-micron thick dry film, MX5050, was laminated on the silicon wafer. This dry film resist was used to promote the adhesion between Au and silicon. Next, the wafer was baked on a hot plate at 100 °C for 1 min followed by exposure to UV light for 45 s. All irradiated samples were exposed to UV light with a Cobilt CA-800 UV mask aligner. Then, the wafer was again baked at 100 °C for 1 min. This silicon wafer (laminated with dry film) was sputter coated with gold on the entire surface using a BIO-RAD E6175 plasma sputter coater. Then a positive photoresist (S1813) layer was spin coated on the silicon wafer using a WS-400B-6NPP/LITE spin coater (Laurell Technologies Corporation). It was soft-baked at 115 °C for 1 min. A photomask (as shown in Figure 2.1) was brought in contact with the wafer, followed by exposure to UV for 1 min. The black portion of the photomask blocked UV and, thus, allowed the positive photoresist to crosslink in these areas, whereas the exposed part did not crosslink. Next, the photomask was removed and the wafer was hard-baked at 115 °C for 1 min. After hard-baking, the positive photoresist was developed using a MF™ CD-26 developer. The part that did not crosslink got stripped, thereby exposing the gold in those areas. After developing, the wafer was dipped in a gold etchant solution to etch away the exposed gold, thus, forming the set of bottom electrodes.

PANI/Au films were formed after fabricating the bottom electrodes. After etching, the wafer was washed with DI water and the positive photoresist was stripped using Dyanostrip 7000. The wafer was again washed with DI water and dried with nitrogen. The thickness of the gold electrodes was measured to be around 3.5 μm. Figure

2.2 shows the bottom electrodes formed on the substrate. The PANI/Au precursor was then drop coated on the electrodes with a volume of 30 to 40 μL at various points. The wafer was exposed to UV for 6 min to form a PANI/Au nanocomposite. The wafer was treated (as described in the section on PANI/Au nanocomposite synthesis) to obtain dry PANI/Au dots. The thickness of the PANI/Au nanocomposite dots was measured to be around 20 μm. The PANI/Au dots are shown in Figure 2.3.

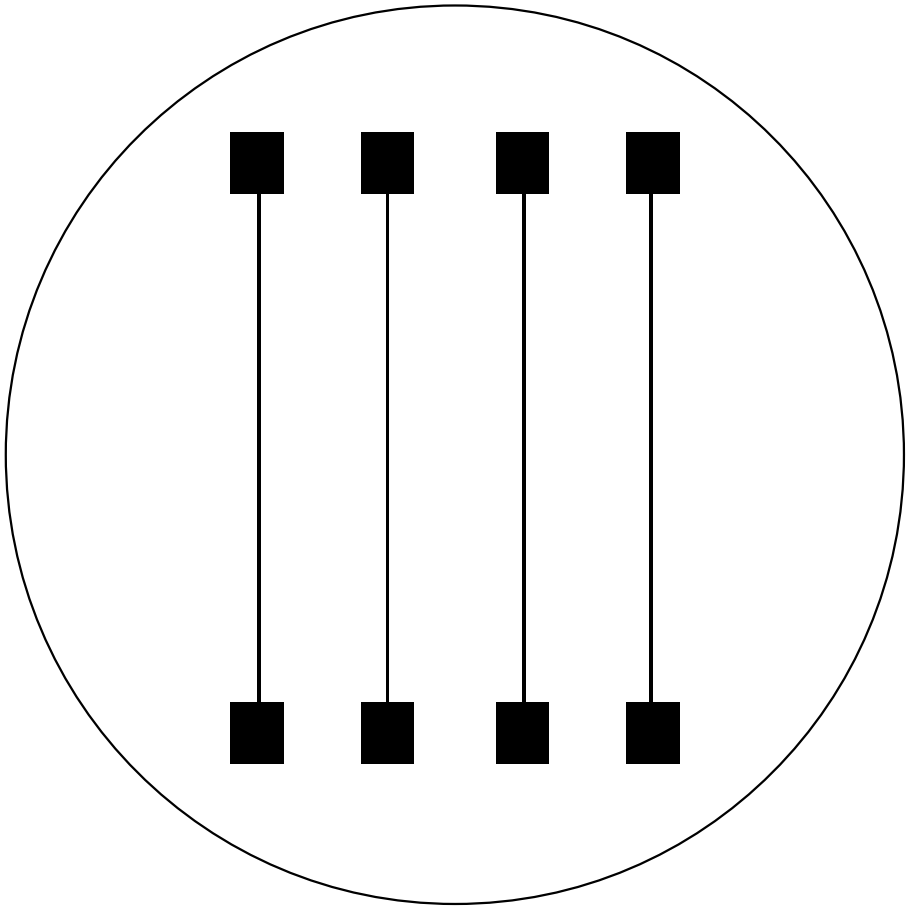

Figure 2.1. Photomask for bottom electrodes using a positive photoresist.

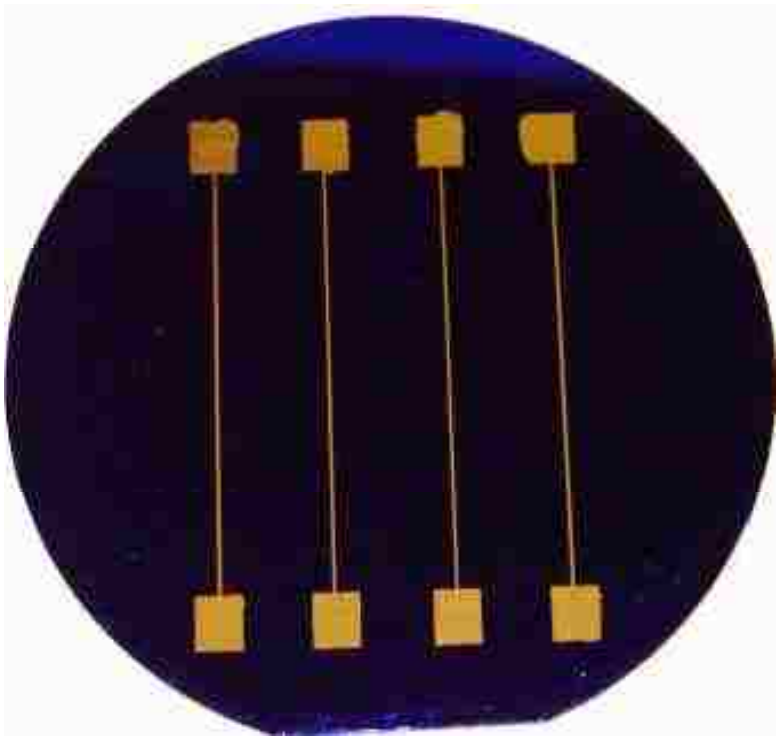

Figure 2.2. Photograph of bottom electrodes on a Silicon wafer laminated with dry film.

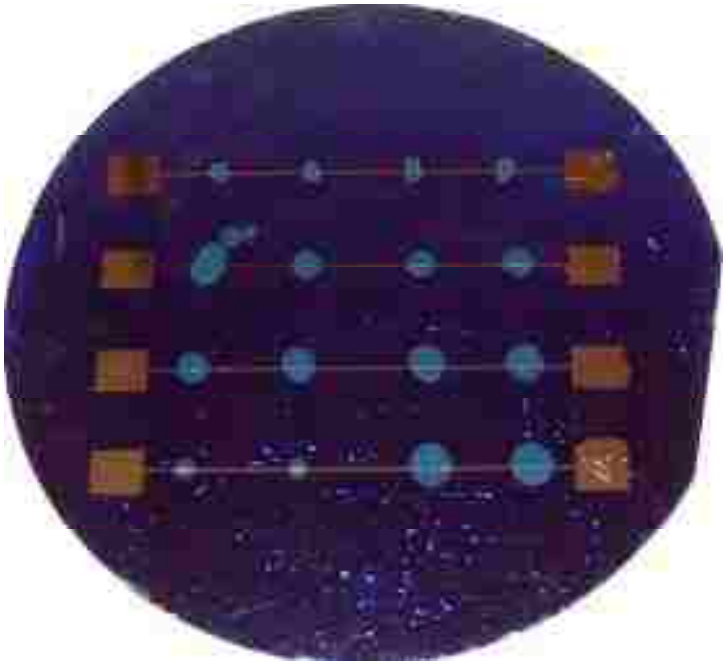

Figure 2.3. Photograph of PANI/Au nanocomposite dots on the bottom electrodes.

A shadow mask was attached to the wafer to form the top electrodes. A photomasking technique was not used to form the top electrodes, as it was not possible to expose the wafer to various chemicals like Au etchant, photoresist strippers and developers due to the presence of the PANI/Au nanocomposite. Thus, an alternate approach of shadow masking was used. Figure 2.4 shows the shadow mask used. Electrodes (represented by the red color) are holes in the shadow mask that allowed the Au plasma to be deposited on the wafer. The electrodes (represented by the black part on the mask) were used to align the mask on the substrate so that the top electrodes were perpendicular to the bottom electrodes, with the PANI/Au layer sandwiched in between. After attaching the shadow mask, the wafer was sputter coated with gold to form the top electrodes. The thickness of these electrodes was measured to be around 1.3 μm. This step completed the device.

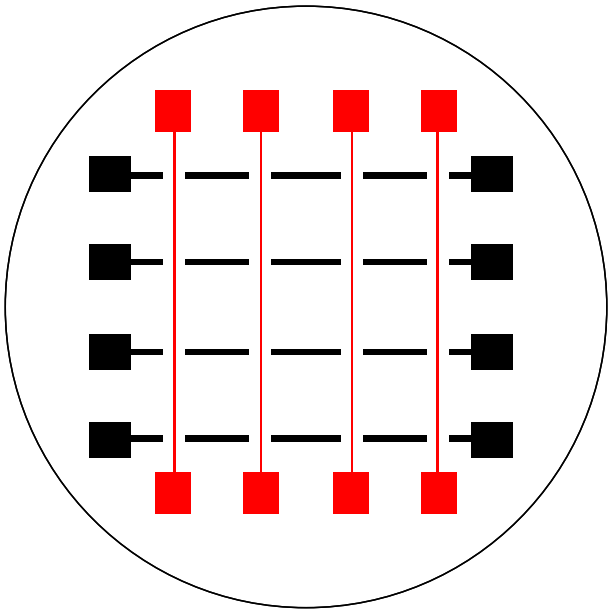

Figure 2.4. Shadow mask for the top electrodes.

Contact pads were attached to connecting wires using silver epoxy, curable at room temperature. Soldering was avoided as heat might degrade the nanocomposite's structure. A photograph of the completed device is shown in Figure 2.5. The electrodes which appear to be vertical in the figure, form the set of top electrodes. The electrodes which appear to be horizontal in the figure, form the set of bottom electrodes. Each intersection of a top and a bottom electrode formed a device where the PANI/Au dot was sandwiched between the electrodes. The width of each electrode was around 300 μm, as per the photomask design. Thus, each device area measured approximately 300 x 300 microns.

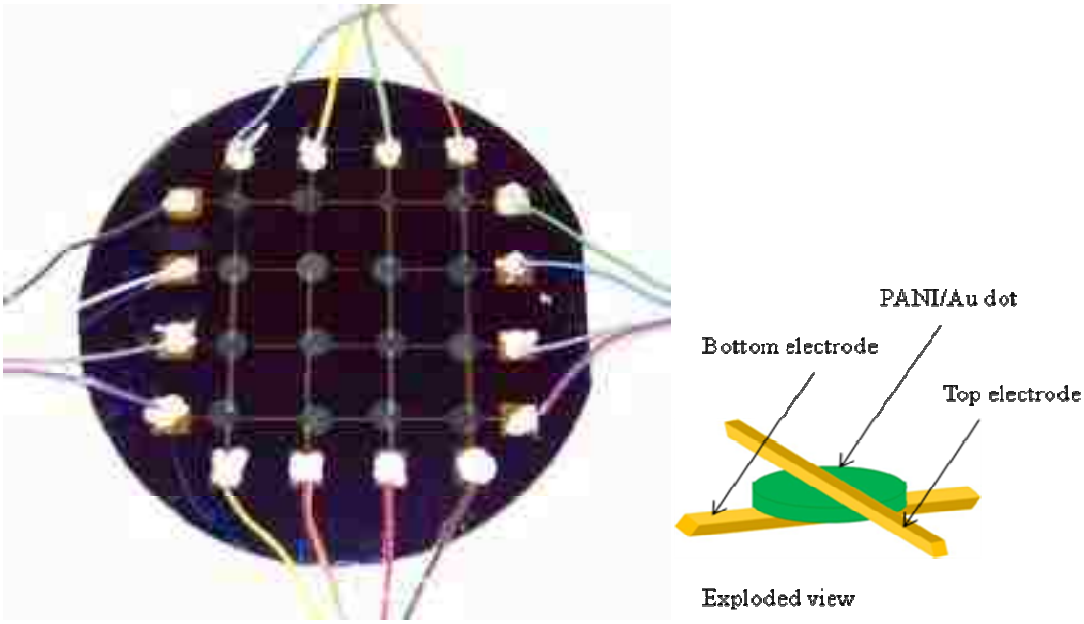

Figure 2.5. Photograph of the completed horizontal device #1 with exploded schematic view of one memory element.

2.2.4.2 Horizontal device #2. This device was also fabricated on a 4-inch Si wafer. A 4-inch silicon wafer was washed in acetone, methanol and DI water, for 3 min in each, to clean the surface impurities. The wafer was spin dried and also heated to 150 °C for 6 min to evaporate the moisture. A thin layer of SU-8 2050 was spin coated on the silicon wafer. It was soft-baked for 6 min at 60 °C and 3 min at 90 °C. The SU-8 layer was then exposed to UV for 1 min for crosslinking. Finally, it was hard-baked for 6 min at 60 °C and 9 min at 90 °C. This SU-8 layer was used, as adhesion of gold on Si is poor. The SU-8 layer was measured to be around 70 μm thick. A thin layer of gold (measured to be around 3.5 μm thick) was sputtered on this SU-8 coated Si wafer using a BioRad E6175 plasma sputter coater. A GE PETE (polyester) filter membrane, of 10-μm thickness, was soaked in a PANI/Au precursor solution and placed on the Au coated Si wafer. It was then irradiated with UV for 6 min and dried/washed/dried, as per the synthesis recipe described in Section 2.2.2. to complete the fabrication of the device.

A small semicircular aluminum electrode on a glass slide was brought in contact with a PANI/Au soaked filter membrane to act as the top electrode. The electrode diameter was designed to be 1.5 mm with a 20 μm thick Al foil. Figure 2.6 is a photograph of the electrode.

Similar devices were constructed using GE CA (cellulose acetate) as well as cloth and paper filter membranes that were much thicker. Filter membranes are porous and act like a template as well as a supporting matrix for the growth of PANI/Au nanocomposites. However, the cloth and paper filter membranes were very thick (measured ~125 μm). It was determined that the thickness of the active PANI/Au layer

affected a device's characteristics and that devices made from thick filter membranes were not useful.

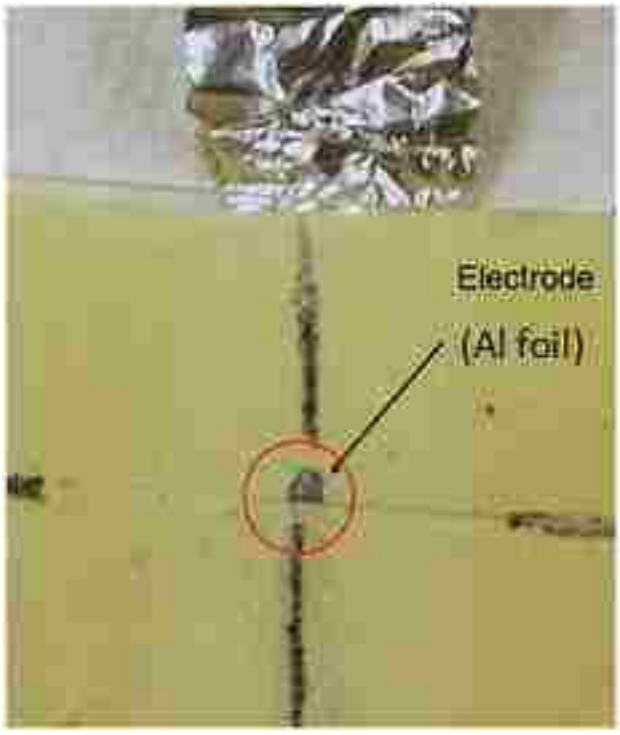

Figure 2.6. Photograph of a top aluminum electrode for horizontal device #2.

2.2.4.3 Horizontal device #3. This device was constructed using portions of the fabrication procedures developed for horizontal devices #1 and #2. A 4-inch silicon wafer was laminated with dry film resist, followed by formation of bottom electrodes, as described in the fabrication procedure for horizontal device #1. Next, a GE PETE filter membrane was soaked in a PANI/Au solution and placed on the fabricated Si wafer, illuminated with UV for 6 min and then dried for 12 h under constant air flow. After

drying, the filter membrane was carefully peeled off of the substrate. The GE PETE membrane was hydrophilic and had a pore size of 10 μm. The filter membrane was placed on the substrate after soaking it in a PANI/Au precursor aqueous solution. The solution started to flow from the pores of the membrane towards the substrate, due to gravity. Next, it flowed between the filter membrane and the substrate due to capillary action. This facilitated formation of a uniform thin liquid film between the membrane and the substrate, which upon exposure to UV, produced a PANI/Au nanocomposite. After drying, the filter membrane was carefully peeled off, leaving a large PANI/Au thin film on the substrate. The film was then washed with DI water and dried for 12 h, completing the fabrication.

The top electrode was built using photolithography on a separate 75 mm x 50 mm glass slide. The glass slide was washed in acetone, methanol and DI water, for 3 min in each, to clean the surface impurities. The glass slide was spin dried and also heated at 150 °C for 6 min to evaporate the moisture. Next, a 50-micron thick dry film, MX5050, was laminated on the glass slide. Dry film resist was used to promote the adhesion between the Au and glass. Next, the slide was baked on a hot plate at 100 °C for 1 min. It was exposed to UV for 45 s. The slide was again baked at 100 °C for 1 min. After this, the entire layer of dry film was crosslinked on the slide, and laminated with another layer of dry film. Next, the slide was baked on a hot plate at 100 °C for 1 min. Then a photomask (shown in Figure 2.7) was attached to the glass slide and the slide was exposed to UV for 45 s. The black portion of the photomask did not allow UV to pass through and, thus, the dry film did not crosslink in those areas. Only fine dots (300 μm in diameter) in this second layer of dry film were crosslinked. The slide was again baked at 100 °C for 1 min.

The dry film was developed using a D-4000 liquid developer, and then washed with DI water. This completed the photoresist coating process.

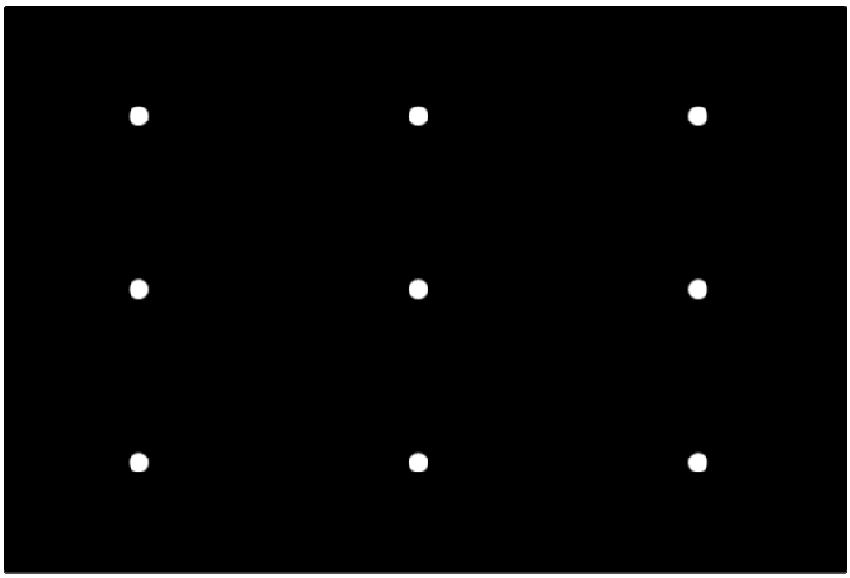

Figure 2.7. Negative photomask for an electrode (figure not to scale).

The glass slide was sputter coated with gold on the entire surface after formation of dry film layers. The diameter of the gold electrode was around 300 microns, as per the photomask design, and the thickness of the electrode was 50 microns (i.e., the thickness of one layer of dry film). Figure 2.8 shows a schematic view of the electrode. Only one electrode was exposed, while the others were covered while taking the readings, so the signal generated represented the current from only a single electrode.

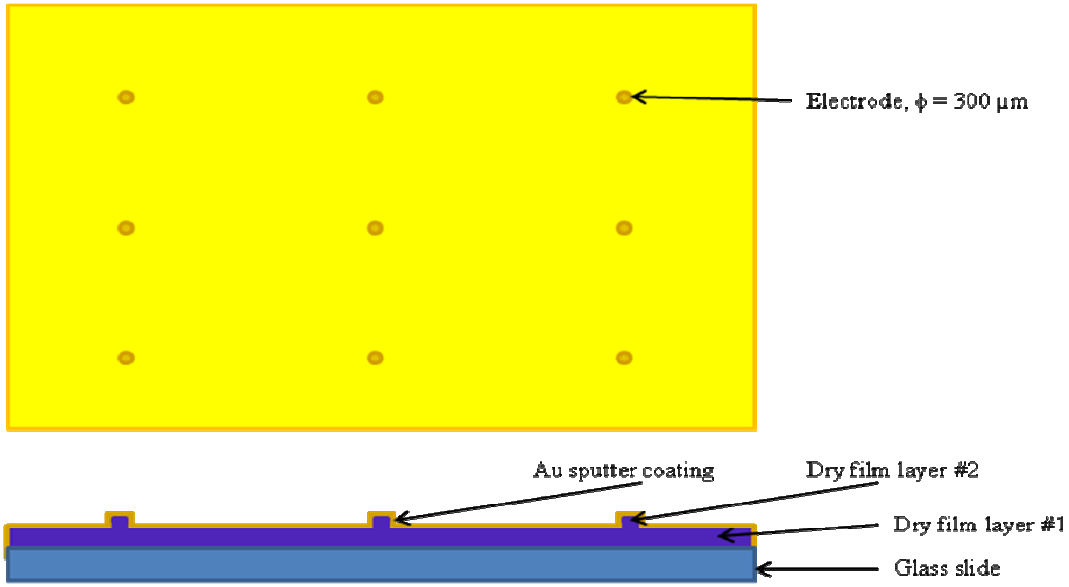

Figure 2.8. Schematic view of a top electrode (figure not to scale).

2.2.4.4 Horizontal device #4. This device was built on a porous flexible plastic substrate. GE PETE (polyester) filter membrane (thickness = 10 micron) was used as the substrate. The plastic filter was soaked in a PANI/Au precursor solution and irradiated with UV for 6 min. It was dried/washed/dried as per the synthesis recipe described in Section 2.3.2. The plastic membrane was porous and helped form a matrix structure for an embedded PANI/Au nanocomposite. Adhesion of the PANI/Au nanocomposite to this membrane was found to be extremely good and the flexible plastic membrane acted as the substrate as well as an active device layer. After formation of the PANI/Au nanocomposite in the membrane, it was sputter coated with Au to form top and bottom electrodes using the shadow masking technique, as described for horizontal device #1. Thus, the membrane contained PANI/Au embedded within it and sputtered gold electrodes on both sides of it that acted as top and bottom electrodes. The device structure

was similar to horizontal device #1, except for the substrate. Figure 2.9 shows the flexible device. The electrodes which are vertical in the figure are the bottom electrodes (on the other side of the filter membrane), whereas the electrodes that are horizontal are the top electrodes.

Figure 2.9. Photograph of a flexible memory device.

2.2.4.5 Horizontal device #5. This device had the simplest structure and was prepared on either a 75 mm x 50 mm or 75 mm x 25 mm glass slide. Figure 2.10 illustrates this type of device. A precleaned glass slide was taken and sputter coated with Au to cover the entire surface. This gold layer served as the bottom electrode, and was measured to be around 2.75 μm thick. Next, the slide was drop coated with a PANI/Au

precursor solution (20 to 50 μL drop size) and exposed to UV for 6 min. After irradiation, it was dried/washed/dried as per the synthesis recipe in Section 2.3.2. Care was taken while washing these devices as the adhesion of gold to glass was not very good and washing lead to breaking or peeling of the gold film a few times. The washing step required extreme care. After final drying, the device was brought in contact with a top electrode. Initial experiments used a top electrode made from aluminum, as described for horizontal device #2. However, a sophisticated top electrode (ϕ = 300 μm) with mechanical screw and gravity-spring action, was created for the later devices.

A schematic view of the sophisticated electrode can be seen in Figure 2.11. This electrode improved the accuracy and reliability of the results by eliminating excess pressure on the PANI/Au film, thus preventing it from being compressed, scratched or broken. The mechanical screw helped lower the electrode slowly to the contact point on the PANI/Au thin film, thereby preventing impact of the electrode and, hence, scratches on the film. Once this electrode touched the PANI/Au film, it rested on the film because of gravity. Even if the screw was lowered, the spring action prevented any additional pressure on the PANI/Au film from the electrode, which still maintained its position on the film. The pressure on the film was always equal to the gravitational force that was acting on the electrode. Copper was used as the top electrode material. Here the PANI/Au film was formed by drop coating. Devices with PANI/Au films, formed using the filter membranes (as described for horizontal device #3) were also made on Au-coated precleaned glass substrates. Spin-coated PANI/Au films were also formed on the Au-coated precleaned glass substrate by spin coating 200 μL of precursor solution at 120 rpm. Devices, with precleaned glass slides directly coated with Au, were preferred as

such a substrate was highly hydrophilic, leading to formation of very thin PANI/Au films (measuring around 1.3 - 3.5 µm).

Figure 2.10. Photograph of drop-coated PANI/Au films on Au-coated precleaned glass.

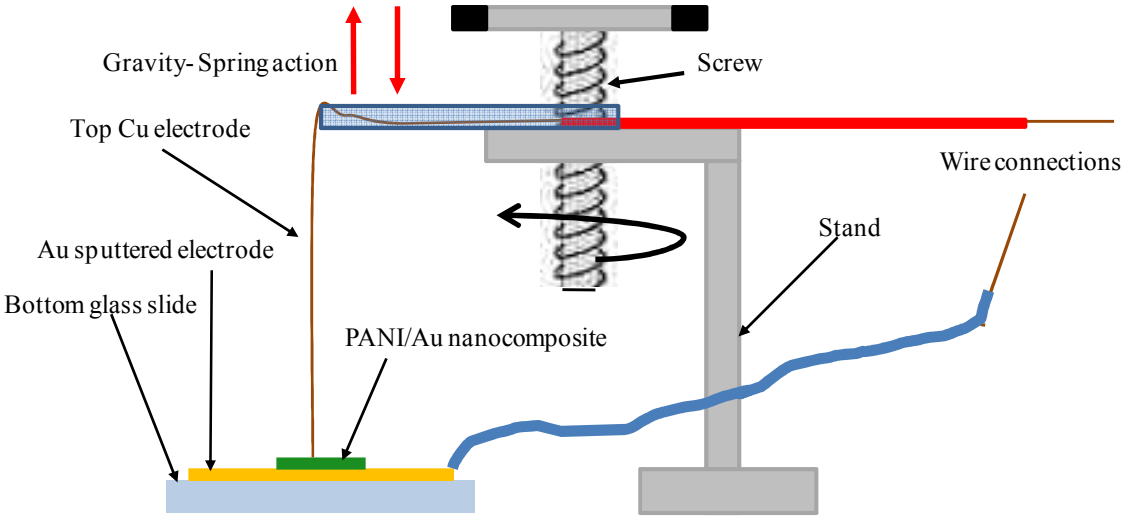

Figure 2.11. Screw and gravity-spring loaded top electrode (figure not to scale).

2.2.4.6 Horizontal device #6. This device was constructed using glass slides. A 75 mm x 50 mm precleaned glass slide was sputtered with Au using the shadow masking

technique (described for horizontal device #1) to form the bottom electrodes. Another precleaned 75 mm x 25 mm glass slide was taken and sputter coated with Au on the entire surface to form the top electrode. However, the sputtering time was considerably less for the top electrode as it had to remain translucent. The thickness of the top electrode was measured to be around 150 nm. A PANI/Au precursor solution was dropped on the bottom glass slide and the top electrode was pressed against the liquid layer. As a result, excess precursor solution oozed out and a thin uniform film of precursor solution was trapped between the electrodes due to capillary action. The device was irradiated with UV for 12 min. The top electrode was glued to the bottom electrode at the edges, after irradiation, to prevent sliding of the electrodes or peeling of the PANI/Au film. After irradiation, the device was dried under constant air flow for 12 h. The thickness of the PANI/Au layer was measured at around 450 nm. Figure 2.12 shows a schematic view of the device.

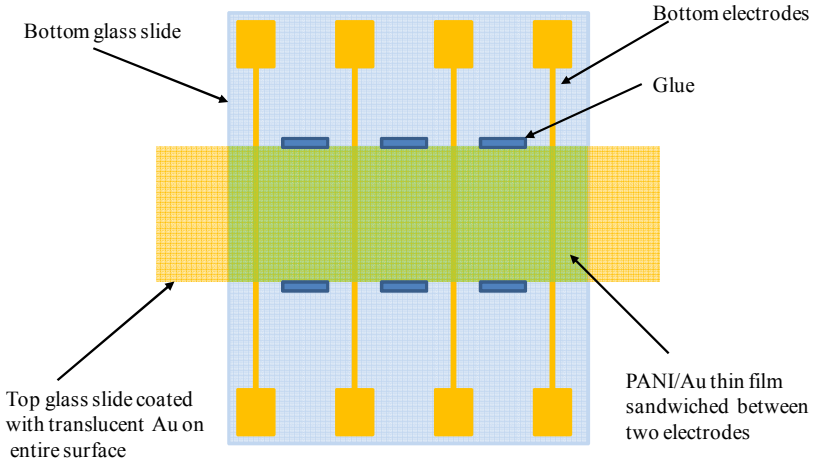

Figure 2.12. A PANI/Au thin film device between two glass slides (figure not to scale).

2.2.5. Vertical Device Fabrication. Glass slides were used to construct the vertical electrode device. Two 75 mm x 25 mm glass slides were washed in acetone, methanol and DI water, for 3 min in each, to clean the surface impurities. Next, they were spin dried, followed by heating at 150 °C for 6 min to evaporate the moisture. Both slides were sputtered with Au, using a shadow masking technique, to make the vertical electrodes and the extensions for contact pads. A PDMS substrate was prepared in a petri dish by mixing a 10:1 ratio of PDMS base to initiator. It was allowed to crosslink for 24 h at atmospheric conditions. The dimension of the vertical electrodes was 5 mm x 2 mm along the thin vertical edges of the glass slides. These electrodes were extended horizontally beyond the vertical edges so that contacts to the connecting wires could be made easily. Figure 2.13 shows an example of the vertical device.

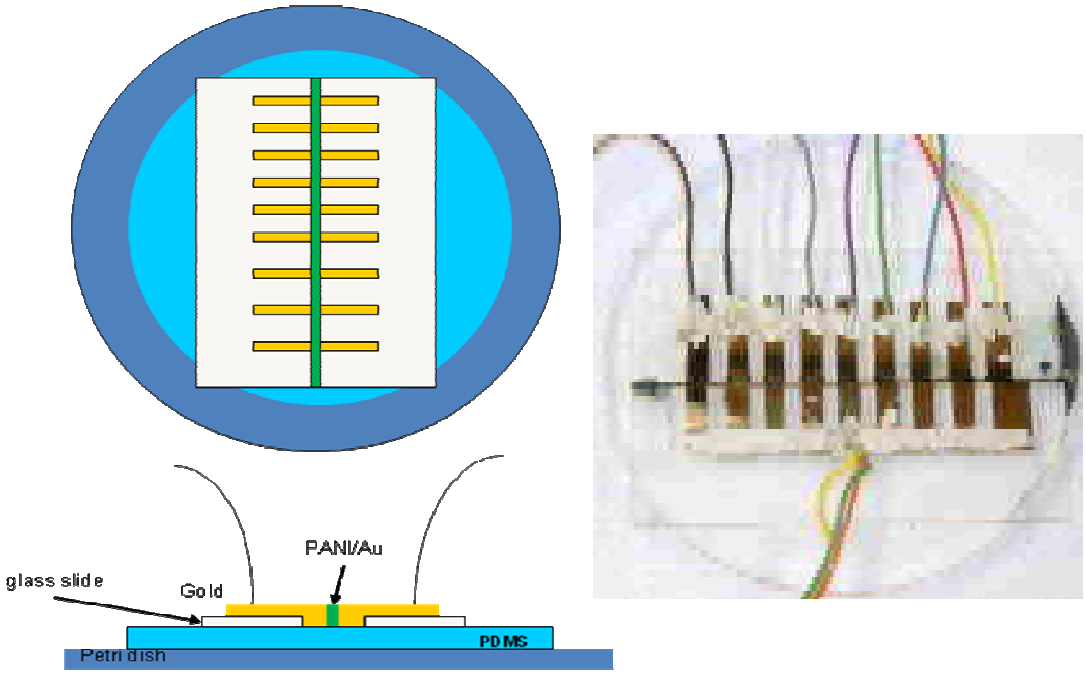

Figure 2.13. Schematic view (not to scale) and photograph of vertical electrode device.

After shadow masking the glass slides, spacers in widths of 10, 20, 50, 100, and 200 μm were used to generate micro-channels of different widths between two glass slides. The effect of gaps between the electrodes on characteristics of the device could then be determined. This entire assembly was built on the PDMS substrate previously formed in a Petri dish.

2.3. RESULTS AND DISCUSSION

Scanning electron microscope (SEM) images of various samples were obtained. Typical bulk PANI/Au morphology, as seen in unirriadiated samples, is represented in Figure 2.14. This morphology is consistent with the formation of bulk PANI that was previously reported by our group.[10,28] ImageJ software (developed at National Institutes of Health, NIH) was used to measure and obtain data from all SEM micrographs. Thus, bulk-like morphology was obtained for samples that were formed under normal conditions (room temperature, pressure, etc.) without any exposure to UV.

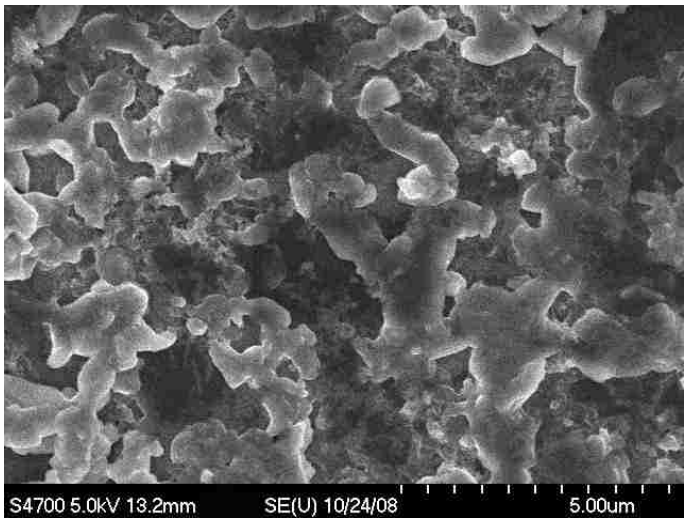

Figure 2.14. SEM image of bulk PANI/Au.

Sample characterization was done by exposing PANI/Au precursor solution to UV for different lengths of time such as 6, 13, and 20 min. All samples were prepared as per the procedure described for horizontal device #2. Figure 2.15 and Figure 2.16 show micrographs of samples exposed to UV for 20 and 13 min, respectively. Nanostructures with diameters ranging from 200 to 250 nm can be seen in both of these micrographs. Samples with an irradiation time of 20 and 13 min did not show any significant differences. This meant that the morphology was not affected by longer exposure times. However, the samples irradiated for 20 or 13 min had higher porosity and larger surface area than bulk samples. Samples irradiated with UV for 6 min showed good nanostructure morphology. Images from different samples (irradiated with UV for 6 min) were obtained and the diameter of nanostructures was found to range from 30 nm to 50 nm. Figure 2.17 shows a highly porous mesh like PANI/Au nanocomposite structure, formed after 6 min of UV exposure. Figure 2.18 shows clear fiber-like morphology for a sample which was dispersed (dilute sonicated sample) for imaging purposes. The fibers appeared to connect together to form mesh-like structures. From various micrographs obtained, it was determined that 6 min was the optimum exposure time as samples irradiated for that amount of time had better nanostructure morphology than samples that were exposed for a longer period of time. Thus, a 6-min exposure time was used for the fabrication of various memory devices.

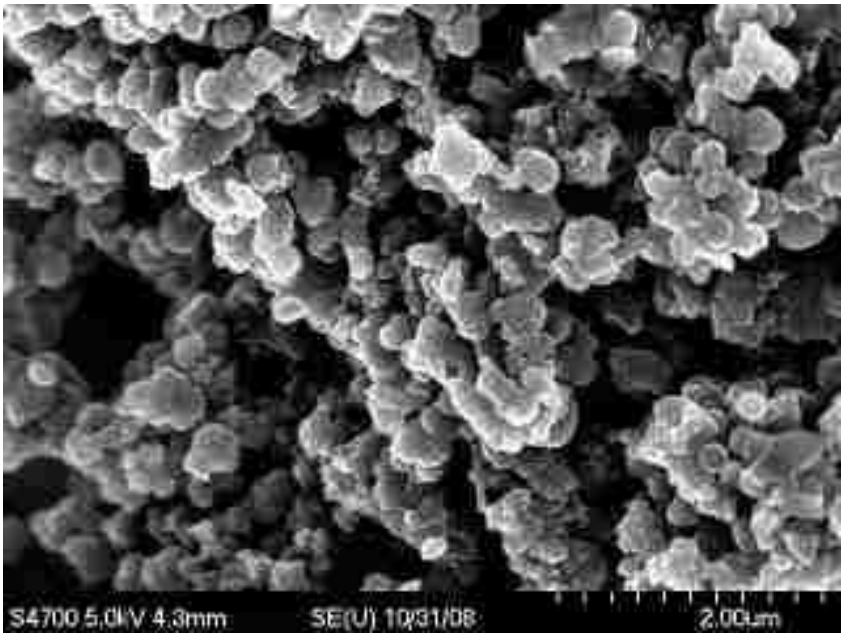

Figure 2.15. SEM image of PANI/Au nanostructures after 20 min of UV exposure.

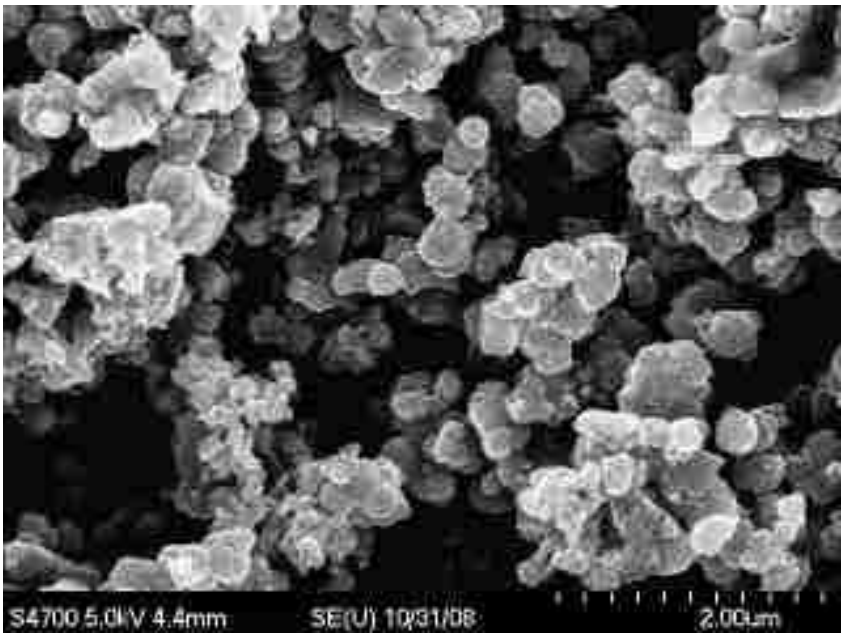

Figure 2.16. SEM image of PANI/Au nanostructures after 13 min of UV exposure.

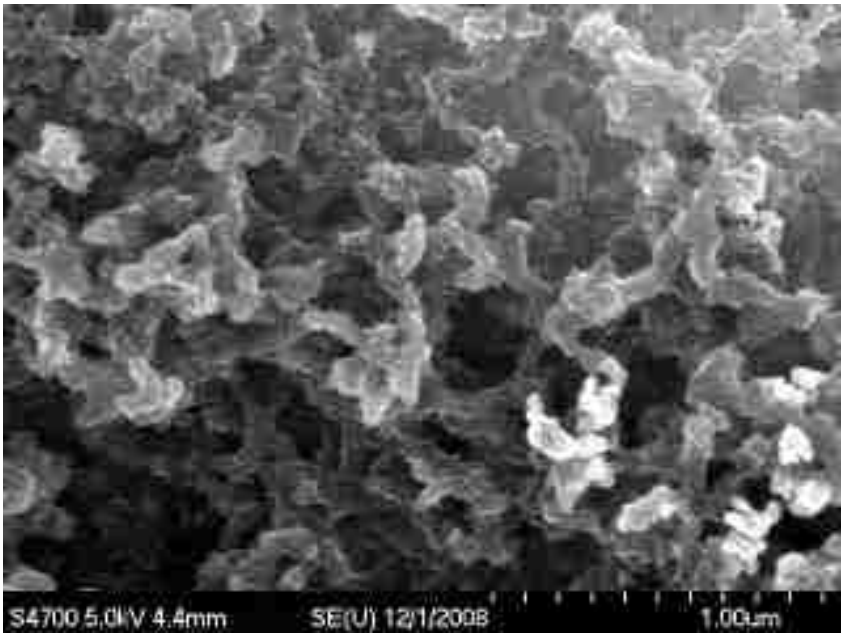

Figure 2.17. SEM image of PANI/Au nanostructures after 6 min of UV exposure.

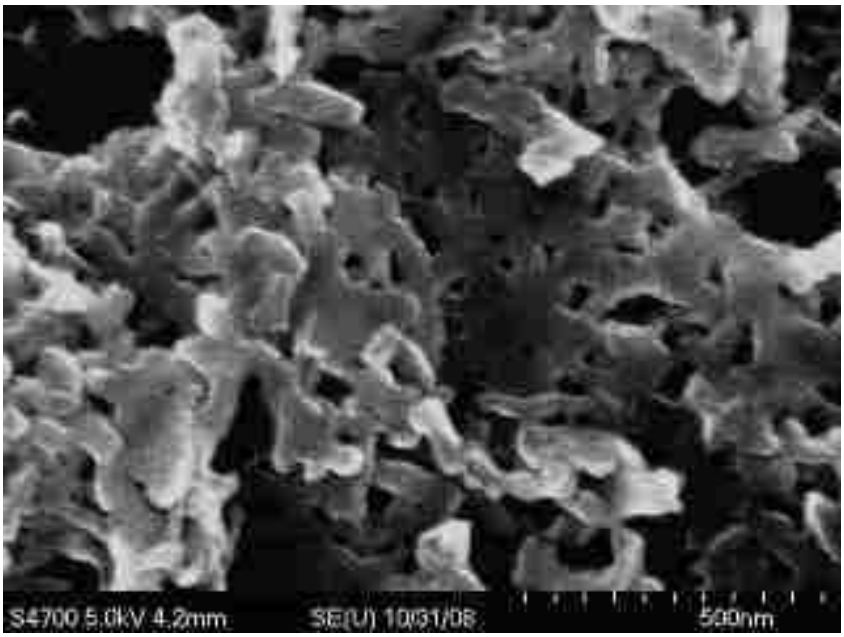

Figure 2.18. SEM image of a dispersed sample of PANI/Au nanostructures after 6 min of UV exposure.

Some regions on the samples exposed to UV for 6 min showed highly dense areas, as illustrated in Figure 2.19. Other portions of the sample showed dense nanofibers that appeared to be attached to each other, forming structures as seen in Figures 2.20 and 2.21. These dense structures may have formed from the fusing of nanofibers. This could happen because of: (1) the decomposition of fibers due to heat and (2) the reaction of unreacted molecules, post irradiation. However, since the samples were carefully maintained at room temperature, this seems unlikely, although localized heating during irradiation due to a photothermal effect was possible. Thus, there may be a small possibility of fusing of nanofibers due to heat. The polymerization reaction of aniline does not need UV to proceed. Thus, after exposure to UV, a large number of unreacted species in the sample can keep reacting thereby altering and fusing the existing nanofibers. Also, if the films were not dried soon after irradiation, it was seen that the film got darker and denser with time, implying the formation of polymer due to reaction after irradiation. Thus, the second reason (growing PANI) may be a major cause for this alteration in morphology, indicating that drying time, post exposure, may be an important factor in maintaining the fiber morphology.

Au particles were not specifically visible in the SEM micrographs. While forming PANI/Au nanocomposite, chloroauric acid itself acts as the oxidant and gets reduced to form gold nanoparticles, thus oxidizing aniline to form polyaniline. As Au nanoparticles were not easily visible in SEM micrographs, it suggested that they should be embedded in the PANI nanostructures. This was verified with TEM micrographs (refer Appendix). In addition, the presence of gold in the sample was verified by TGA.

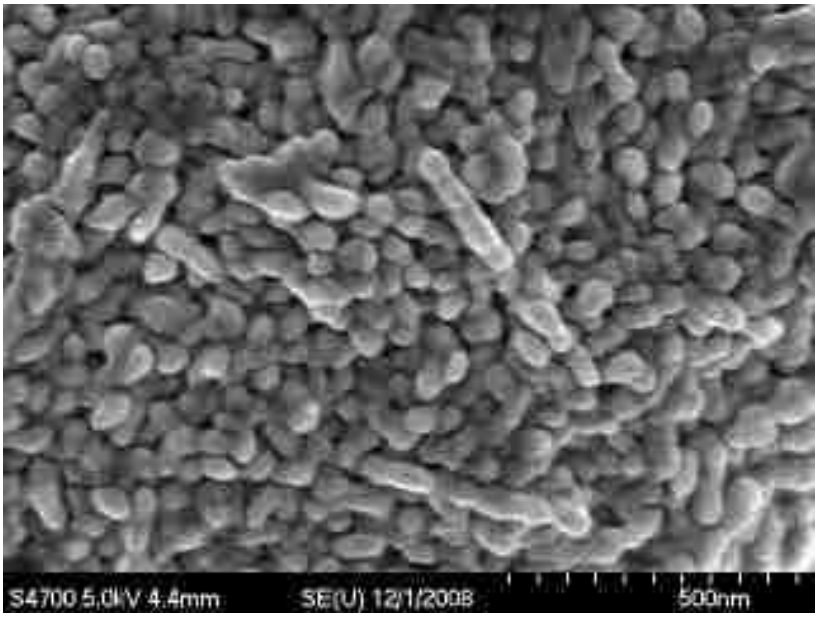

Figure 2.19. SEM image of a dense area of PANI/Au after 6 min of UV exposure.

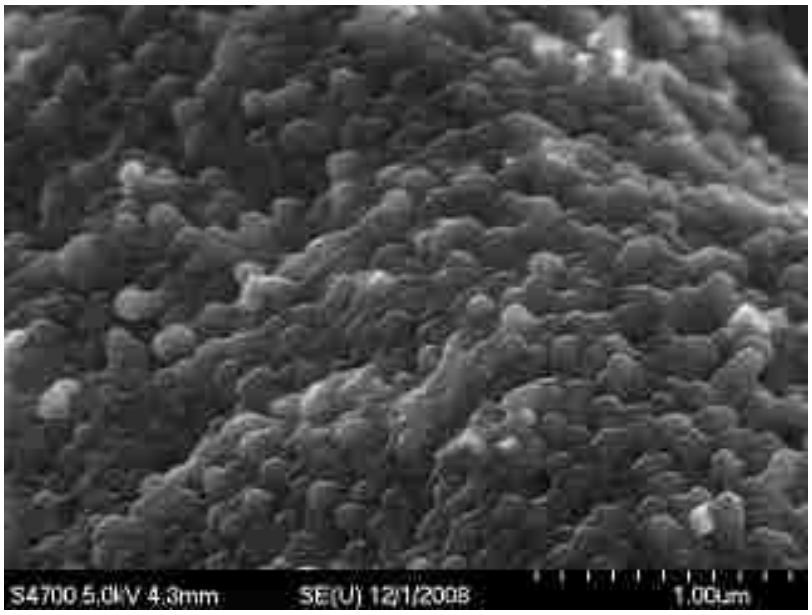

Figure 2.20. SEM image of fused PANI/Au nanostructures with 6 min of UV exposure.

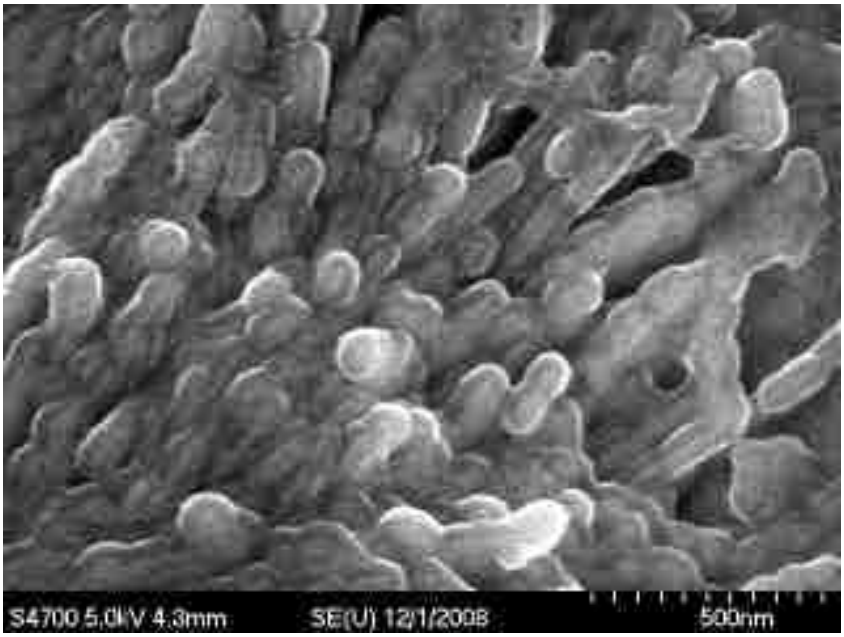

Figure 2.21. High magnification SEM image of fused PANI/Au nanostructures with 6 min of UV exposure.

Thermogravimetric analysis (TGA) was performed on PANI/Au nanocomposite samples that were formed using different ratios of aniline to $HAuCl_4$. This analysis gave an understanding of the final ratio of polymer to Au in the samples. Figure 2.22 shows TGA curves for samples with an initial $HAuCl_4$ concentration of 0.01 M (sample #1), 0.02 M (samples #2), 0.03 M (sample #3) and 0.05 M (sample #4). All samples had an initial aniline concentration of 0.1 M. Loss in mass until a temperature of 100 °C was due to the loss of water, while a loss in mass until 290 °C was reached was due to the loss of dopant. Polyaniline started decomposing at 290 °C and was almost completely decomposed by 600 °C.[29] The remainder of the sample was the metal (gold).

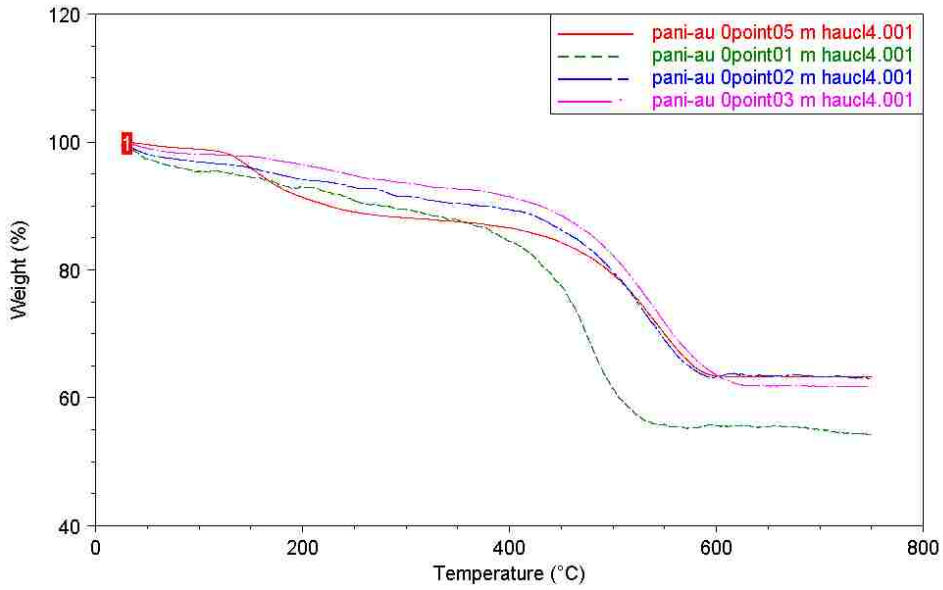

Figure 2.22. Thermogravimetric analysis of PANI/Au nanocomposite samples.

As seen from the thermogram (Figure 2.22), approximately 55% of sample #1 was gold by weight whereas approximately 63% of samples #2, #3 and #4 were gold by weight. On an average, approximately 30 % of all the samples (by weight) were polyaniline. With the initial molar ratios of Au/Aniline ranging from 0.1 to 0.5 in various samples, the final molar ratio of Au/PANI (based on aniline) was about 0.92, on an average. This implies that our method of making PANI/Au nanocomposite is superior in terms of obtaining a high gold to PANI ratio in the product (PANI/Au sample) as compared to other methods previously reported in the literature, even when much lower Au/PANI ratios were used in the precursor solutions.[30]

Contact angle measurements were made of the various substrates used to make different devices noted in this paper. The results are shown in Figure 2.23. It was found that the contact angle between water and the Au coating on precleaned glass slides was 5°

(lowest contact angle, highest hydrophilic surface). On other substrates, however, such as a cleaned glass slide, Si wafer, Si wafer coated with dry film resist, and Si wafer coated with SU-8 photoresist (with a coating of Au on each type of substrate); the contact angle was 30°, 28°, 39° and 45°, respectively. Figure 2.24 shows how the contact angle was measured. From these measurements, it was clear that the Au-coated precleaned glass slide had the highest hydrophilic surface and was the best for making PANI/Au memory devices as it would facilitate formation of thinner nanocomposite films.

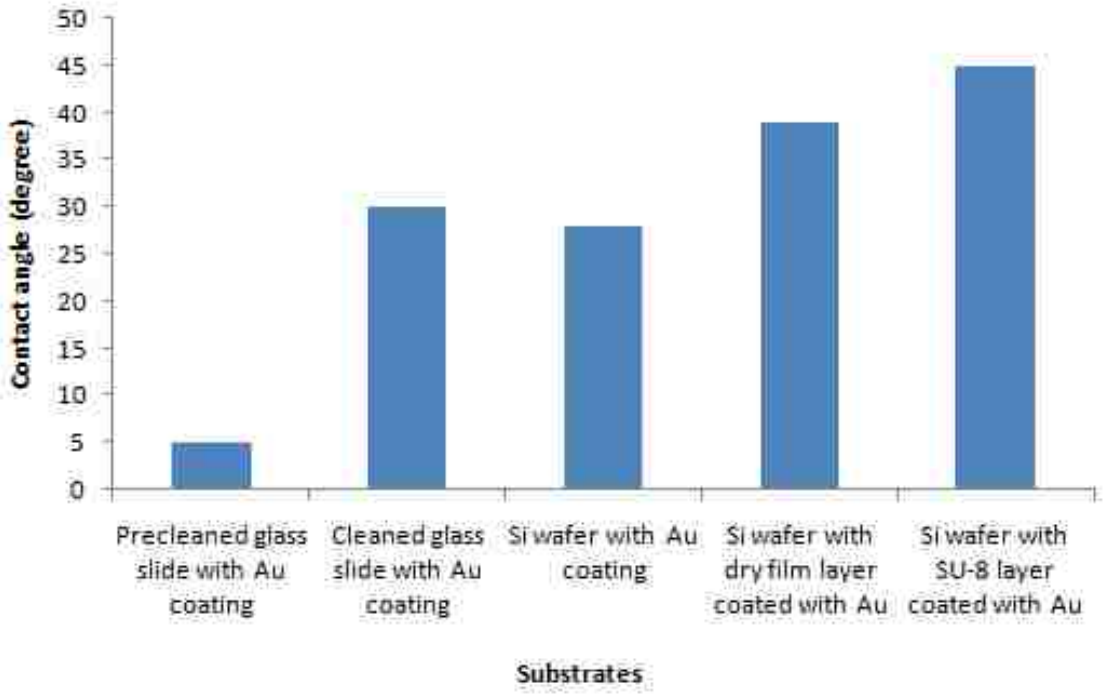

Figure 2.23. Contact angle measurements of various substrates used for memory devices.

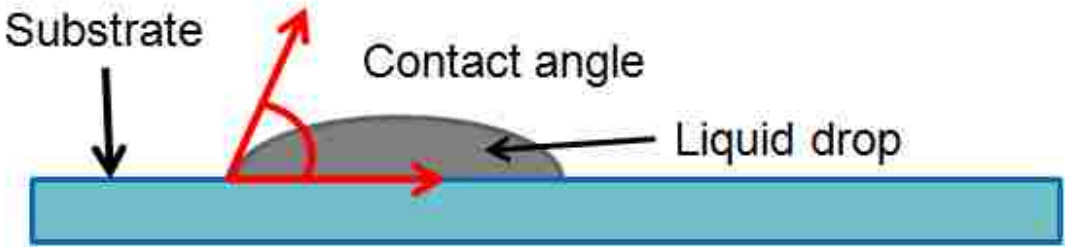

Figure 2.24. Contact angle measurement method.

Various fabrication methods were used to make PANI/Au nanocomposite memory devices. Many of the devices made using these fabrication techniques did not show reproducible and sufficient memory-like behavior.

Horizontal device #1 made use of a large number of microfabrication steps and is closest to the industrially used microfabrication procedures for semiconductive devices. This was one of the good things about this device. However, the contact angle on this substrate was much higher, leading to a higher film thickness. Also, the difficulty in sputter coating the top electrodes at a controlled sputtering rate (with BIORAD E6175 plasma sputter coater) made it difficult to control the thickness of the top electrode above the PANI/Au film as well as the depth of Au penetration in the PANI/Au matrix during sputter coating the top electrodes. The device did not show a memory effect and showed current similar to the OFF state characteristics, perhaps to due to the above mentioned processing difficulties.

Horizontal device #2 was made using various filter membranes on top of a SU-8 coated Si wafer with Au sputtered bottom electrode. The filter papers proved to be good as far as adhesion of PANI/Au nanocomposite was concerned. They provided a

supporting matrix for the nanocomposite to grow. However, the filter papers were too thick with some of them being as thick as around 125 μm. The devices were unable to show a memory effect implying that the film thickness was probably too high for such a memory device.

Horizontal device #3 was made using a thin film formed under the porous filter membrane. It was difficult to obtain a uniform thin film of PANI/Au under the filter membrane. In some of the regions, the film was completely absent. As adhesion of PANI/Au on the filter membrane was good, while peeling of the filter membrane, some of these areas on the film remained attached to the filter membrane instead of the Si substrate. This device did show result a few times, but they were not reproducible enough for a reliable memory device.

Horizontal device #4, constructed on a porous polyester filter membrane, shows a method of making flexible memory devices. The adhesion of PANI/Au to this membrane was extremely good. However, this device did not exhibit any memory like behavior. The thickness of the filter membrane was around 10 μm, which seemed to be too high for this PANI/Au device to show any memory like behavior.

Horizontal device #5 had the simplest structure and required a fewer number of fabrication steps compared to all other devices. This device showed promising results, indicating memory-like characteristics. Contact angle measurements support the results shown by horizontal device #5 by showing that contact angles on substrates (other than the precleaned glass slide coated with Au) were much larger. Larger contact angles resulted in larger PANI/Au nanocomposite film thickness. Thus, devices fabricated on

other substrates did not show results indicating that PANI/Au film thickness might have an important effect on the device characteristics.

Horizontal device #6 was made using a thin PANI/Au film between two glass slides. One of the glass slides had extremely thin translucent gold sputter coating on it to act as the top electrode as well as to allow UV to pass through during the irradiation process, facilitating the formation of PANI/Au nanocomposite. However, the resistance of the top as well as the bottom electrode was found to be too high. This high electrode resistance, increased the overall resistance of the circuit and hence this device was unable to show a memory effect.

Vertical device was made with different spacers in between the two electrodes to form microchannels of different widths. However, the microchannel width was too high for the device to function effectively. It was also very difficult to make these microchannels of uniform width throughout using a spacer manually. When the PANI/Au precursor solution was injected into the microchannel and irradiated, it was seen that the nanocomposite that formed, could flow in the microchannel during the handling of the sample by the time it completely dried. This made PANI/Au nanocomposite concentration uneven along the length of the channel. Also, since only small percentage of the actual precursor solution converts into the nanocomposite (major volume of the precursor solution was water), the microchannel was left almost empty with a very little of its volume being occupied by the nanofibers. Thus, these nanofibers were not properly attached to the electrodes, resulting in no contact in some areas. Also, in the areas where there was contact, it did not show any memory effect.

Devices (horizontal device #5) made from PANI/Au nanocomposites on a precleaned glass slide with Au coating exhibited behavior like that of a bistable memory device when a voltage scan was applied to it. At a particular voltage (transition voltage), a sudden increase in the current was observed. All measurements were made under atmospheric conditions and no special conditions, such as vacuum, were used. Differences in current of up to three orders of magnitude between the OFF state and the ON state current were recorded for some of the devices. Figure 2.25 shows the characteristics of a device made on a precleaned glass slide coated with Au (bottom electrode), with an initial $HAuCl_4$ concentration of 0.05 M. The current appears to be saturated in the graph as it was above the range of the instrument (Keithley 617 programmable electrometer). However, the current likely changed with voltage after the transition into the ON state.

The device was stable in the ON state, even after the potential was reduced to zero. This is represented in Figure 2.26 which shows a voltage scan after the device was switched to the ON state. It can be seen that, even when the voltage was scanned from 0 V, the current was always in the larger magnitude region. Again, the current becomes saturated in the graph as it was above the range of the device. The higher conductivity of the ON state can be changed back to the OFF state by applying a negative voltage pulse of around – 5 V. The device remained stable in the OFF state until a voltage equal to or greater than the transition voltage was applied. Figure 2.27 shows a graph of the same device with a positive as well as a negative voltage scan. It can be seen from the figure that the device shows two states (OFF state and ON state) on both the sides of the scan, indicating that the device can be operated sufficiently even after interchanging the

polarity of the electrode terminals. However, as seen from the figure, there was a small difference in the transition voltage and current magnitude on opposite sides of the scan for many of the devices. Some devices did exhibit a negative differential resistance (NDR) in the ON state. Figure 2.28 shows a graph representing the negative differential resistance region on a device made on precleaned glass slide with Au bottom electrode and initial $HAuCl_4$ concentration of 0.04 M. Negative differential resistance has been reported elsewhere in memory devices.[20]

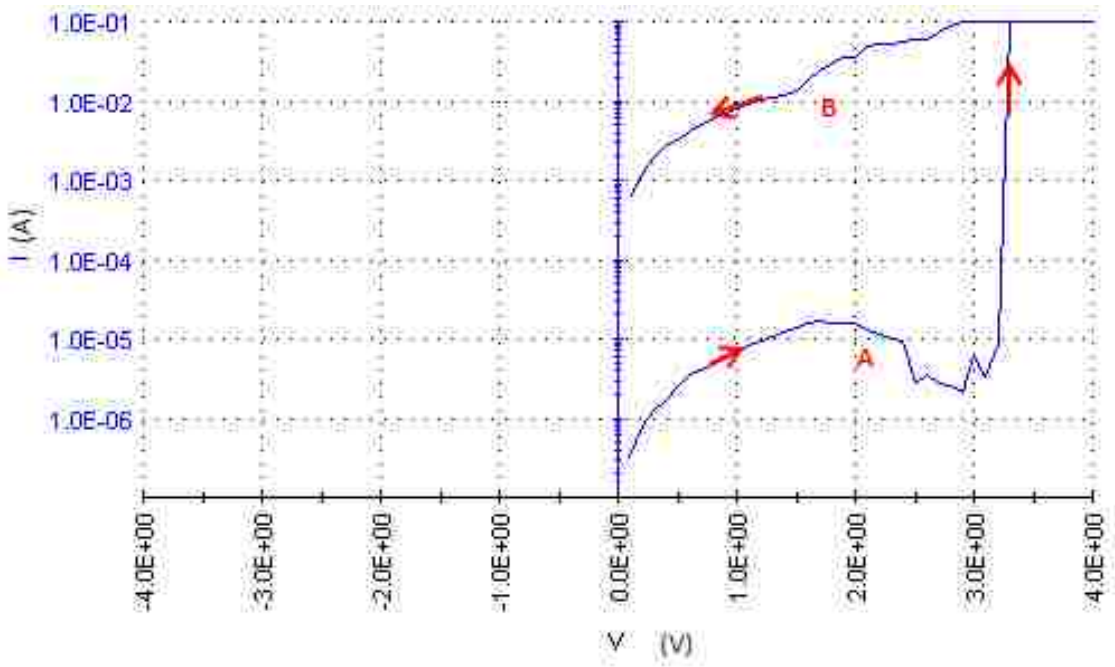

Figure 2.25. Current voltage characteristics of the PANI/Au nanocomposite memory device on a precleaned glass slide with an Au sputter coating: initial $HAuCl_4$ concentration of 0.05 M and transition voltage of around 3.2 V.

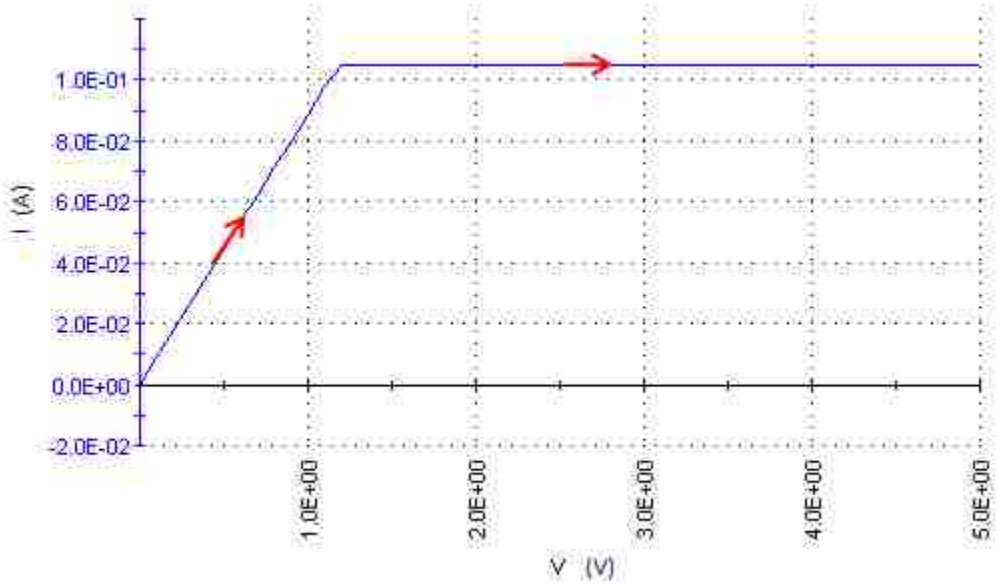

Figure 2.26. Voltage scan (PANI/Au nanocomposite memory device on a precleaned glass slide with an Au sputter coating: initial $HAuCl_4$ concentration of 0.05 M) after switching the device to the ON state.

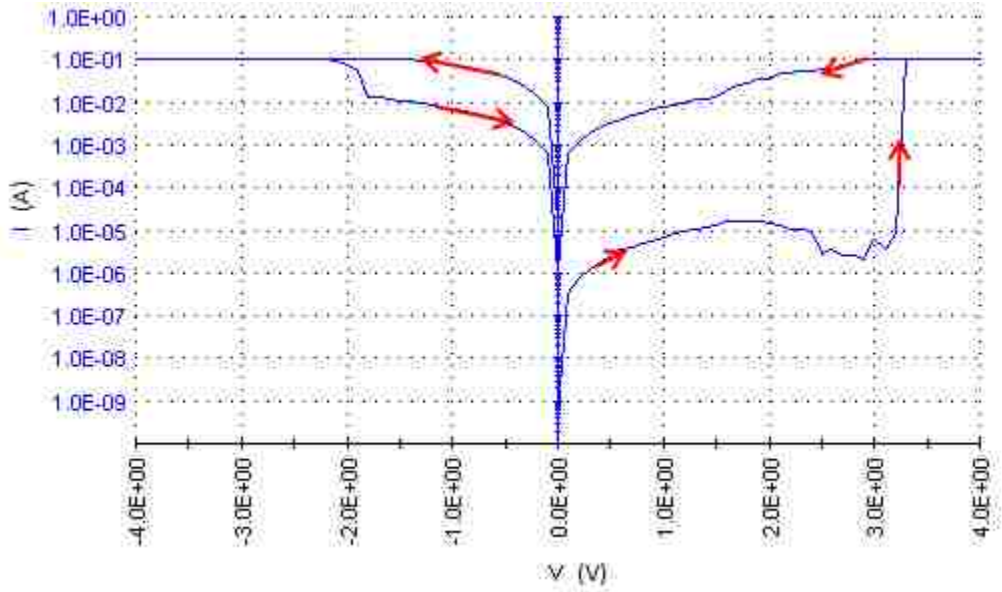

Figure 2.27. Current voltage characteristics of the PANI/Au nanocomposite memory device on a precleaned glass slide with an Au sputter coating: initial $HAuCl_4$ concentration of 0.05 M and with a positive as well as a negative voltage scan.

Various devices, which were made from PANI/Au nanocomposites, showed the characteristics of a memory device. However, devices made from bulk PANI/Au samples did not exhibit such a transitional behavior. For the devices made from a PANI/Au nanocomposite, the magnitude difference in the ON state current and the OFF state current varied from around 500 to 5000, whereas the transition voltage varied between 2 to 3.5 V. Figure 2.29 shows a graph representing device characteristics obtained from another device made on precleaned glass slide with an Au coating on it with an initial $HAuCl_4$ concentration of 0.03 M. Typical average resistance of the device in the OFF state was found to be around 100 k Ω, whereas it was found to be around 150 Ω in the ON state. All of the working devices could be repeatedly used under atmospheric conditions.

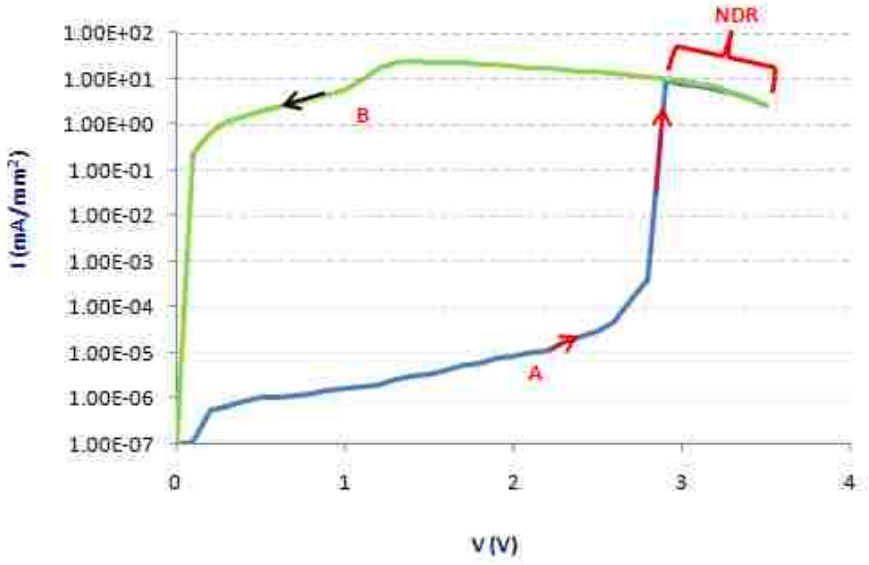

Figure 2.28. Current voltage characteristics of a PANI/Au nanocomposite memory device on a precleaned glass slide with an Au sputter coating: initial $HAuCl_4$ concentration of 0.04 M exhibiting a negative differential resistance region (NDR) after transition voltage (2.9 V).

The transition that occurs from the OFF state to the ON state has been addressed in literature as an electric field-induced charge transfer between gold nanoparticles and PANI nanofibers.[13,30] When the voltage is increased, the electric field between the electrodes increases, and at a threshold electric field, the electrons on the imine nitrogen group of PANI nanofibers gain enough energy to jump to the gold nanoparticles' valence band leading to charge tunneling during the ON state. This redistribution of charges changes the conductance and, hence, shows a large increase in the current. It has been previously reported in literature that, due to strong interactions between the metal nanoparticles and the polymer at the interface, the nanoparticles exhibit a non-metallic behavior due to reduction in the density of states near the Fermi level.[22,31] The voltage at which this charge transfer takes places is called the transition voltage. Thus, use of metallic nanoparticles help to dramatically changes the properties of the polymer films due to their charge storage.[19,20,22]

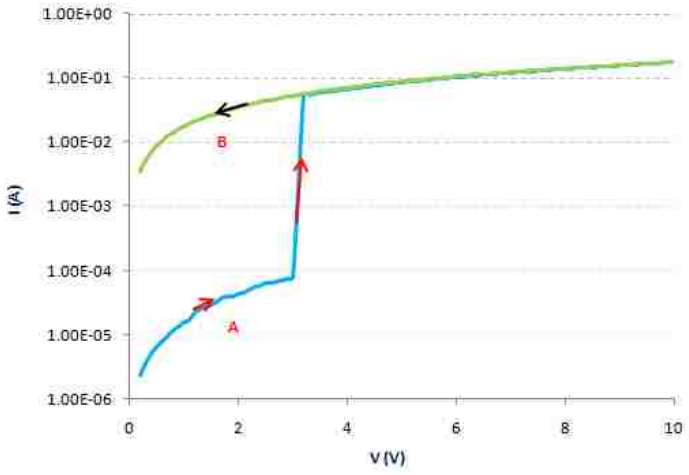

Figure 2.29. Current vs voltage characteristics of a memory device with an initial $HAuCl_4$ concentration of 0.03 M and a transition voltage of around 3.0 V.

2.4. EFFECTIVE CYCLE TIME ANALYSIS

A production cycle analysis for horizontal device #1 was done, which was one of the most time consuming, requiring a large number of wafer fabrication steps using lithographic methods. Figure 2.30 shows a material flow diagram of that process. A total of 26 steps are required for the fabrication of this device. As seen from flow diagram in that figure, the lead time for processing one wafer through the complete process is 137 min and 35 s (i.e. 2 hours 17 min and 35 s). As seen from the flow diagram, the 2nd wafer can enter the process after the 1st wafer is washed in acetone for 3 min. Thus, there continues to be a lag of 3 min between consecutive wafers until they reach the gold sputtering step. Though the moisture evaporation step on the hot plate takes 6 min, it does not increase the lag time between consecutive wafers, as it can process multiple wafers at the same time, with each wafer being independently controlled.

There is a maximum inventory time of 9 min which some of the wafers will spend before entering the sputtering machine. The sputtering machine can process three wafers at a time, but all three wafers must enter and exit the machine at the same time. After sputtering, the positive photoresist is spin coated, which takes 1 min. The spin coater can handle only one wafer at a time, so, a lag of 1 min is introduced between two consecutive wafers. The positive photoresist developing, gold etching, positive photoresist stripping and nitrogen drying steps do not increase the time lag as they have the capacity for to process multiple wafers independently. After that, the wafer spends 2.5 min plus 20 s before being irradiated under UV. The irradiation step takes 6 min, thereby introducing a 6-min time lag between consecutive wafers.

Finally, the wafers reach the sputter machine, before which a wafer might spend a maximum inventory time of 7 min. Three wafers are processed together for 10 min in the sputter machine. Thus, every 10 min, three completely processed Si wafers with 16 memory devices can be manufactured. In other words, it takes 10 min to manufacture 48 memory devices. It should be noted that physical constraints like the number of hot plates, number of sputter machines, number of people working on machines etc. have been ignored for the ease of calculations. Thus, an overall effective cycle time can be said to be 12.5 s. This means that, at every 12.5 s, this kind of production system will give an output of one complete memory device. With a working day of 8 hours, it is possible to produce 2,304 memory devices in a day. It should be noted that these devices are bulky in structure, as per design. Even a slight optimization of the design will dramatically increase the number of devices that can be produced. From this first principle analysis, it can be seen that even the laboratory process is extremely efficient for continuous production as compared to some other processes in literature, which require several hours to produce devices.[13,14] Also, typically millions of transistors may exist on a semiconductor memory device made from Si wafers. With PANI/Au nanocomposite devices having the capacity to go to down to a few nanometers in dimensions, there exists a vast opportunity of scalability and building a comparable process which can be equivalent to or better than the existing process of manufacturing Si memory elements. Thus, there exists a potential for a wide scope of improvement and scalability in this process for mass production at the industrial level with modification of equipment and use of lean manufacturing principles. This can be regarded as one of the most important advantages of our method of fabrication.

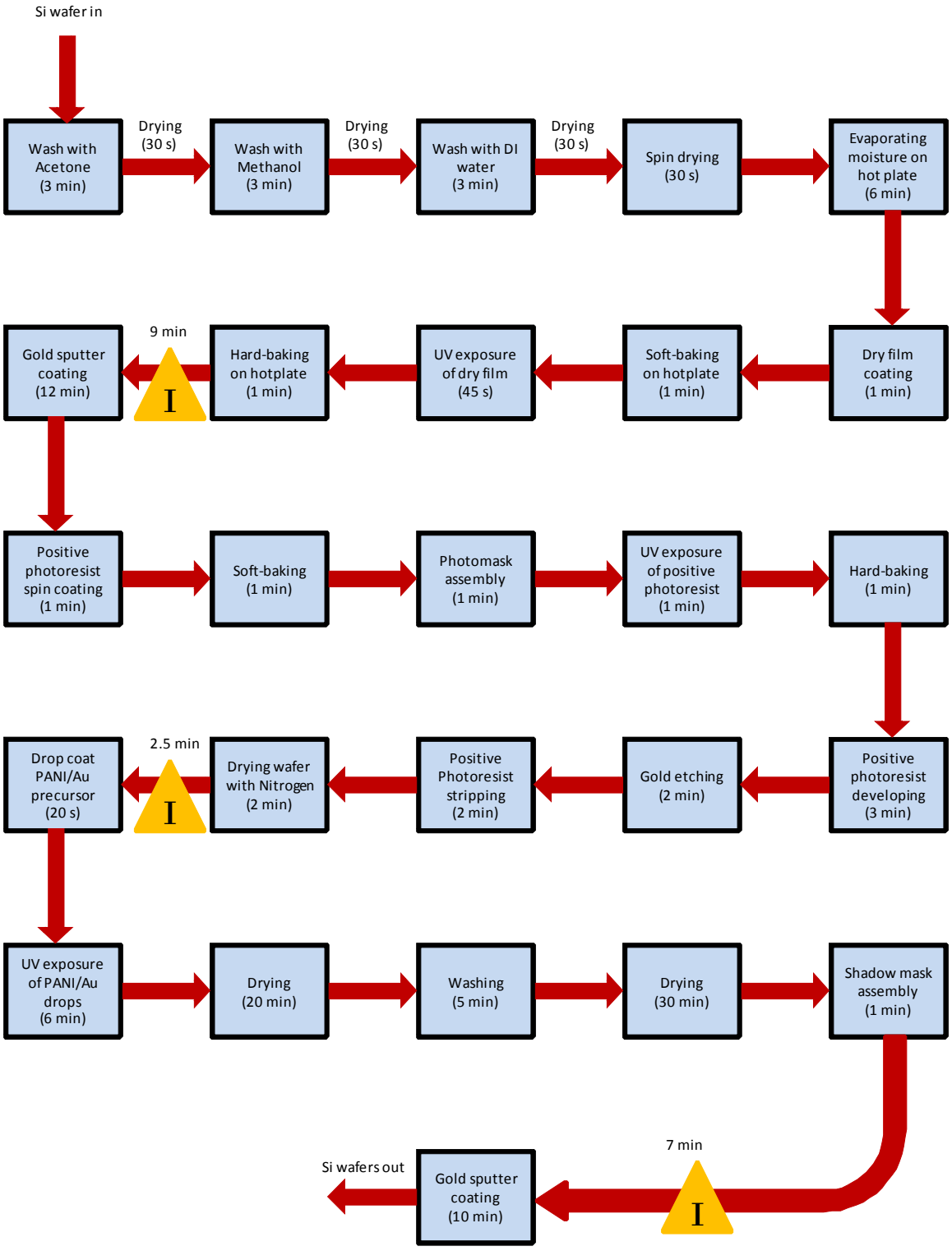

Figure 2.30. Material flow diagram for horizontal device #1.

2.5. CONCLUSIONS

It can be concluded that by using our group's technique of one-step, one-pot synthesis of PANI/Au nanocomposites, it is possible to fabricate a device that has the characteristics of a memory. Our device can work in atmospheric conditions and does not need special conditions like a high vacuum, as required for other PANI/Au memory devices.[13] Our process, being only one-step, is a very easy and cheap method for producing PANI/Au nanocomposites, as compared to other methods described in literature.[13,14] One-pot synthesis enables us to make devices faster and right on the required substrate.

The cycle time analysis of our current laboratory process (for the device requiring maximum number of fabrication steps) with an overall effective cycle time of 12.5 s, indicates a huge potential for such a process being feasible for mass production at the industrial level. Also, our process is highly scalable because of the way this process was designed. Many new technologies developed through research make an important contribution to science, but may not be feasible for industrial mass production. These kind of technologies might prove ineffective for making commercial products usable for future generations. However, our method of fabricating a PANI/Au nanocomposite based memory device, including the PANI/Au synthesis, certainly appears to be suitable for future industrial-level mass production.

Our devices have been able to show large magnitudes of difference (as large as ~5000) between the OFF state and the ON state current. Also, a lot of devices had transition voltages of between 2 to 3.5 V, which is comparable to existing semiconductive memory devices. The methods of fabrication demonstrated in this paper

include rigid as well as flexible substrates. Future work in this area will include fine tuning of the parameters affecting the characteristics and performance of memory devices so that more reliable and reproducible results can be obtained. Fine tuning of these parameters will enable successful fabrication of memory devices, even on flexible substrates with required current vs voltage characteristics.

2.6. ACKNOWLEDGEMENT

The authors acknowledge the financial support of the National Science Foundation under grant DMR-0706197 (FDB) and the Missouri University of Science and Technology.

2.7. REFERENCES

1. Heeger, A. J.; *Rev Modern Phys.* **2001**, 73, 681.
2. Gardner, J. W.; Bartlett, P. N. *Sensors Actuators A* **1995**, 51, 57.
3. Yu, G.; Gao, J.; Hummelen, J. C.; Wudl, F.; Heeger A. J. *Science* **1995**, 270, 1789.
4. Brabec, C. J.; Sariciftci, N. S.; Hummelen, J. C. *Adv. Funct. Mater*. **2001**, 11, 15.
5. Sariciftci, N. S.; Smilowitz, L.; Heeger, A. J.; Wudl, F. *Science* **1992**, 258, 1474.
6. Huang, J. X.; Virji, S.; Weiller, B. H.; Kaner, R. B. *J. Am. Chem. Soc.* **2003**, 125, 314.
7. Virji, S.; Huang, J. X.; Kaner, R. B.; Weiller, B. H. *Nano Lett*. **2004**, 4, 491.
8. Debarnot, D. N.; Epaillard, F. P. *Analytica Chimica Acta* **2003**, 475, 1.
9. Sutar, D. S.; Padma, N.; Aswal, D. K.; Deshpande, S. K.; Gupta, S. K.; Yakhmi, J. V. *Sensors Actuators B* **2007**, 128, 286.
10. Li, Z. F.; Blum; F. D.; Bertino, M. F.; Kim, C. S.; Pillalamarri, S. K. *Sensors Actuators B* **2008**, 134, 31.
11. Smela, E.; Mattes, B. R. *Synthetic Metals.* **2005**, 151, 43.

12. Baker, C. O.; Shedd, B.; Innis, P. C.; Whitten, P. G.; Spinks, G. M.; Wallace, G. G.; Kaner, R. B. *Adv. Mat.* **2008**, 20, 155.

13. Tseng, R. J.; Huang, J. X.; Ouyang, J.; Kaner, R. B.; Yang, Y. *Nano Lett*. **2005**, 5 1077.

14. Li, L.; Ling, Q. D.; Zhu, C.; Chan, D. S. H.; Kang, E. T.; Neoha K. G. *J. Elect. Soc*. **2008**, 155, H205.

15. Wei, D.; Baral, J. K.; Österbacka, R.; Ivaska, A. *J. Mat. Chem*. **2008**, 18, 53.

16. Scott, J. C. *Science* **2004**, 304, 62.

17. Chen, Y.; Ohlberg, D. A. A.; Li, X.; Stewart, D. R.; Williams, R. S.; Jeppesen, J. O.; Nielsen, K. A.; Stoddart, J. F.; Olynick, D. L.; Anderson, E. *Appl. Phys. Lett*. **2003**, 82, 1610.

18. Ma, L. P.; Liu, J.; Yang, Y. *Appl. Phys. Lett*. **2002**, 80, 2997.

19. Ma, L. P.; Pyo, S.; Ouyang, J.; Xu, Q. F.; Yang, Y. *Appl. Phys. Lett*. **2003**, 82, 1419.

20. Bozano, L. D.; Kean, B. W.; Deline, V. R.; Salem, J. R.; Scott, J. C. *Appl. Phys. Lett*. **2004**, 84, 607.

21. Ouyang, J.; Chu, C. W.; Szmanda, C. R.; Ma, L. P.; Yang, Y. *Nat. Mater*. **2004**, 3, 918.

22. Wu, J.; Ma, L. P.; Yang, Y. *Phys. Rev. B* **2004**, 69, 115321.

23. Friend, R. H.; Gymer, R. W.; Holmes, A. B.; Burroughes, J. H.; Marks, R. N.; Taliani, C.; Bradley, D. D. C.; Dos Santos, D. A.; Bre´das, J. L.; Lögdlund, M.; Salaneck, W. R. *Nature* **1999**, 397, 121.

24. Müller, C. D.; Falcou, A.; Reckefuss, N.; Rojahn, M.; Wiederhirn, V.; Rudati, P.; Frohne, H.; Nuyken, O.; Becher, H.; Meerholz, K. *Nature* **2003**, 421, 829.

25. Ma, L; Yang, Y. *Appl. Phys. Lett*. **2004**, 85, 5084.

26. Sirringhuas, H.; Tessler, N.; Friend, R. H. *Science* **1998**, 280, 1741.

27. Dimitrakopoulos, C. D.; Mascaro, D. J. *IBM J. Res. Dev*. **2001**, 45, 11.

28. Werake, L. K.; Story, J. G.; Bertino, M. F.; Pillalamarri, S. K.; Blum, F. D. *Nanotech*. **2005**, 16, 2833.

29. Kulkarni, M. V; Viswanath, A. K. *J. Macromol. Sci. Pure Appl. Chem*. **2004**, 41, 1173.

30. Tseng, R. J.; Baker, C. O.; Shedd, B.; Huang, J.; Kaner, R. B.; Ouyang, J.; Yang, Y. *App. Phys. Lett*. **2007**, 90, 053103.

31. Boyen, H. G.; Ziemann, P.; Wiedwald, U.; Ivanova, V.; Kolb, D. M.; Sakong, S.; Gross, A.; Romanyuk, A.; Uttner, M. B.; Oelhafen, P. *Nat. Mater*. **2006**, 5, 394.

3. ONE-POT SYNTHESIS OF A MEMORY DEVICE USING POLYANILINE AND GOLD NANOCOMPOSITES

Krunal R. Waghela[1], Frank D. Blum[2], Chang-Soo Kim[3], Massimo F. Bertino[4]

[1]Department of Chemical and Biological Engineering, Missouri S&T, Rolla, MO 65409

[2]Department of Chemistry and Department of Materials Science and Engineering, Missouri S&T, Rolla, MO 65409

[3]Department of Electrical and Computer Engineering, Department of Biological Sciences, Missouri S&T, Rolla, MO 65409

[4]Department of Physics, Virginia Commonwealth University, Richmond, VA 23284

3.1. ABSTRACT

Fabrication of a memory device using one-step/one-pot synthesis for making a PANI (polyaniline)/Au nanocomposite is reported. These devices showed a bistable behavior, which is typical of memory devices. The ratio of the current in the OFF state to the current in the ON state was seen to be as high as 5000. The basic structure used consisted of a PANI/Au thin film sandwiched between two electrodes. The PANI/Au nanocomposite thin film was constructed right on the electrode with the application of ultraviolet irradiation. PANI nanostructures were found to be around 30 to 50 nm in diameter. $HAuCl_4 \bullet 3H_2O$ was used as a source for the Au nanoparticles. Chloroauric acid

oxidizes aniline and becomes reduced to form Au nanoparticles, thus making the reaction possible in one step. The fabrication technique discussed in this paper is highly scalable for mass production at an industrial scale implying that PANI/Au nanocomposite based memory devices can be readily manufactured by using traditional methods of microfabrication used for making semiconductive electronic memory devices.

3.2. INTRODUCTION

Electrically conductive polymers have opened up a new horizon because their properties can be superior to traditional semiconductors.[1,2] Thus, these conjugated polymers may possibly replace traditional semiconductors in a number of electronic devices. It has already been shown that conducting polymers can be used to make devices like solar cells,[3-5] sensors,[6-10] actuators,[11-12] memory devices,[13-22] light emitting diodes,[23-24] and transistors.[25-27]

Polyaniline is one of several conductive polymers that have been studied extensively. Several researchers have attempted to make memory devices using polyaniline.[13-15] However, because a large number of steps are required in these procedures to fabricate the devices,[13-15] an extremely long time is consumed using these processes to produce multiple devices. Processes that can be scaled up for mass production and that require significantly fewer steps (and thus less time) are desirable for industrial and commercial applications.

Our research group has already shown that microfabrication techniques can be used to make thin films of PANI nanofibers and nanocomposites using one-step/one-pot synthesis through UV irradiation.[10,28] These thin films are extremely suitable for semiconductor applications. This paper describes one of the techniques that can be used

to fabricate a memory device using one-step/one-pot synthesis with the application of UV irradiation. The synthesis of PANI/Au nanocomposites can be performed directly on the electrode assembly and the device can be ready to use soon after polymerization. These devices were tested to determine if their characteristics included a suitable memory effect. Our fabrication technique was used to produce PANI/Au nanocomposite-based memory devices.

3.3. EXPERIMENTAL

The overall device fabrication consists of fabricating the electrodes, followed by PANI/Au nanocomposite thin film synthesis.

3.3.1. Materials. Aniline and $HAuCl_4 \bullet 3H_2O$ were obtained from Alfa Aesar, and HCl was obtained from Fisher Scientific. All chemicals were used as received, except aniline, which was distilled before use. 75 mm x 25 mm x 1mm plain precleaned micro glass slides were obtained from Dow Corning.

3.3.2. Polyaniline/Gold Nanocomposite Synthesis. Typically, to prepare the PANI/Au nanocomposites, two 5 ml solutions were mixed. One solution consisted of 5 ml of deionized (DI) water, 94 µl aniline and 330 µl of 37% HCl in a vial. Another solution consisted of 5 ml of DI water and chloroauric acid in another vial. Various concentrations of $HAuCl_4 \bullet 3H_2O$ ranging from 0.01 M to 0.05 M were used for different samples. Reactants in both the vials were mixed together to form a precursor solution with 10 ml of DI water, 94 µL aniline (0.1 M), 0.3 M HCl and $HAuCl_4 \bullet 3H_2O$ in a vial. $HAuCl_4$, which acted as the oxidant for aniline, was reduced in the process to form Au nanoparticles. The addition of chloroauric acid started the polymerization reaction.

3.3.3. Characterization. All experiments to measure the current characteristics of the memory devices were conducted at room temperature and at atmospheric pressure. The current-voltage curves for the memory device were measured using a Keithley 617 programmable electrometer and a Keithley 4200SCS semiconductor parameter characterization system. The morphology of PANI/Au nanocomposites was characterized using Hitachi S-4700 scanning electron microscope (SEM). The thicknesses of the various PANI/Au samples on the devices were measured using a Tencor Alpha-Step 200 and thermogravimetric analysis (TGA) was used to determine the amount of Au in the sample. TGA measurements were made with air flowing at 100 cc/min and a ramp rate of 20 °C/min with a Hi-Res TGA 2950 thermogravimetric analyzer.

3.3.4. Horizontal Device Fabrication. The device used had a simple structure and was prepared on either a 75 mm x 50 mm x 1 mm or 75 mm x 25 mm x 1 mm glass slide. Figure 3.1 illustrates this device. A precleaned glass slide was sputter coated with Au to cover the entire surface. This gold layer, around 2.75 μm thick, served as the bottom electrode. The slide was then drop coated with a PANI/Au precursor solution as described previously (20 to 50 μL drop size) and exposed to UV (365 nm – 5.4 mW/cm^2, 405 nm – 13 mW/cm^2, Cobilt CA-800 UV mask aligner) for 6 min. After irradiation, the samples were dried under a constant air flow for about 4 to 5 h. After drying, the samples were washed with acetone and DI water to remove the unreacted species, and again put under constant air flow for 12 h before being tested. The washing of these devices was done with extreme care as the adhesion of gold to glass was not very good and washing occasionally led to breaking or peeling of the gold film. Devices, with precleaned glass

slides directly coated with Au, were preferred as such a substrate was highly hydrophilic, leading to formation of very thin PANI/Au films (measuring around 1.3 - 3.5 μm).

After final drying, the device was brought into contact with a top electrode which was made from copper. A complex top electrode (diameter ϕ = 300 μm), with a mechanical screw and gravity-spring action, was created. A schematic view of this electrode can be seen in Figure 3.2. The mechanical screw helped lower the top electrode slowly to the contact point on the PANI/Au thin film. It also prevented strong impact of the electrode and, hence, scratches on the film. Once this electrode touched the PANI/Au film, it rested on the film because of gravity. Even if the screw was lowered, the spring action prevented any additional pressure on the PANI/Au film from the electrode, which still maintained its position on the film. For practical purposes, the pressure on the film was always equal to the gravitational force that was acting on the electrode.

Figure 3.1. Photograph of drop-coated PANI/Au films on Au-coated precleaned glass.

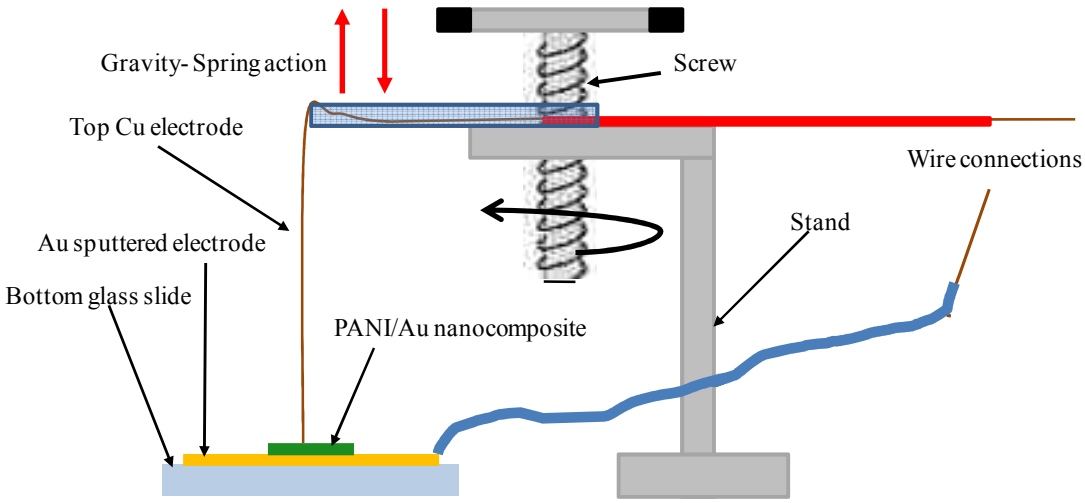

Figure 3.2. Screw and gravity-spring loaded top electrode (figure not to scale).

3.4. RESULTS AND DISCUSSION

Scanning electron microscope (SEM) images of various samples were obtained. Samples irradiated with UV for 6 min showed good nanofiber morphology. Images from different samples (irradiated with UV for 6 min) were obtained and the diameters of nanofibers were found to range from 30 nm to 50 nm, consistent with our earlier work.[10,28] Figure 3.3 shows a highly porous mesh-like PANI/Au nanocomposite structure, formed after 6 min of UV exposure.

Thermogravimetric analysis (TGA) was performed on PANI/Au nanocomposite samples that were formed using different ratios of aniline to $HAuCl_4$. On average, approximately 30 % of all the samples (by weight) was polyaniline. With the initial molar ratios of Au/aniline ranging from 0.1 to 0.5 in various samples, the final molar ratio of Au/PANI (based on aniline) was about 0.92, on an average. This implies that our method

of making PANI/Au nanocomposite is effective at incorporating large fractions of gold in the sample, as compared to other methods previously reported in the literature.[29]

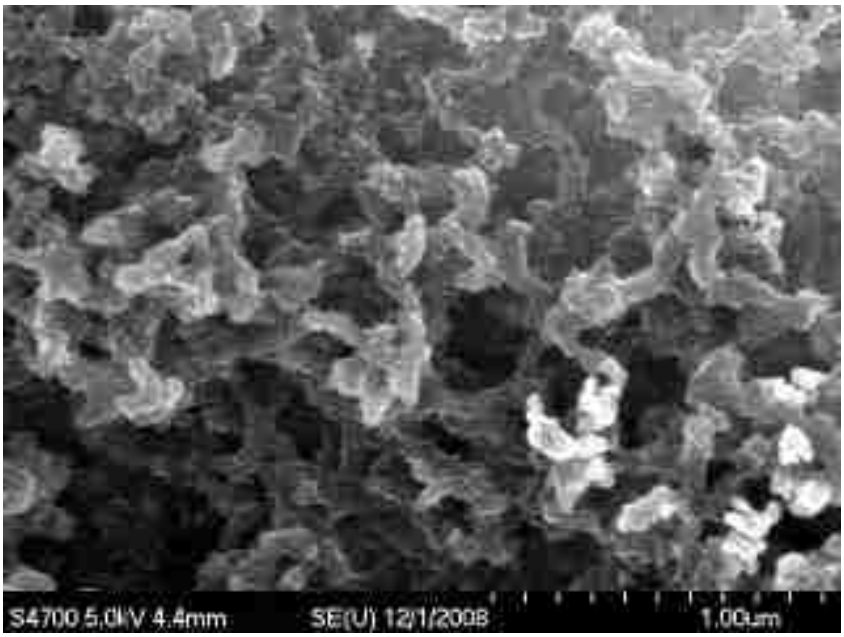

Figure 3.3. SEM image of PANI/Au nanostructures after 6 min of UV exposure.

Devices made from PANI/Au nanocomposites on a precleaned glass slide with Au coating exhibited behavior like that of a bistable memory device when a voltage scan was applied to them. At a particular voltage, the transition voltage, a sudden increase in the current was observed. Differences in current of up to three orders of magnitude between the OFF state and the ON state current were recorded for some of the devices. Figure 3.4 shows the characteristics of a device made on a precleaned glass slide coated with a Au bottom electrode. The initial $HAuCl_4$ concentration for this sample was 0.05

M. The current appeared to be saturated in the graph because it became greater than the working range of the instrument (Keithley 617 programmable electrometer). Even though the current above 100 mA appeared flat due to instrument limitations, it was changing with voltage after the transition into the ON state.

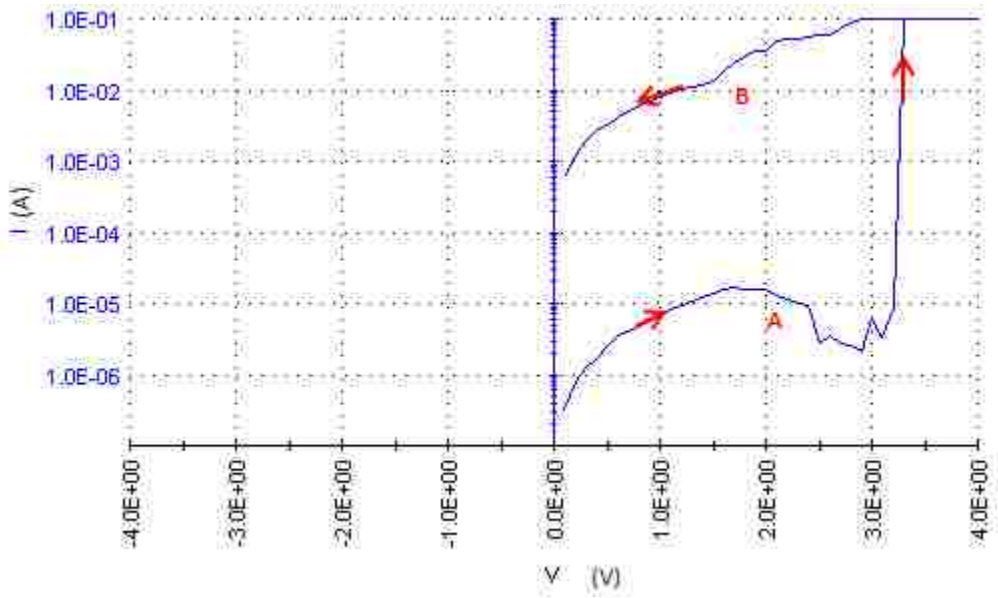

Figure 3.4. Current voltage characteristics of the PANI/Au nanocomposite memory device on a precleaned glass slide with an Au sputter coating: initial $HAuCl_4$ concentration of 0.05 M and transition voltage of around 3.2 V.

To check the stability of the device in the ON state, the voltage was reduced to zero and then a positive voltage scan was done starting from 0 V. The device was stable in the ON state, even after the potential was reduced to zero. This is represented in Figure 3.5 which shows a voltage scan after the device was switched to the ON state. It can be seen that, even when the voltage was scanned from 0 V, the current was always in the

higher magnitude (lower resistance) region. The initial current appears to follow Ohm's law until it reached the instrument limit. The higher conductivity of the ON state can be changed back to the OFF state by applying a negative voltage pulse of around – 5 V. The device remained stable in the OFF state until a voltage equal to or greater than the transition voltage was applied. Some devices did exhibit a negative differential resistance (NDR) in the ON state.[13] Figure 3.6 shows a graph representing the negative differential resistance region on a device made on a precleaned glass slide with a Au bottom electrode and an initial $HAuCl_4$ concentration. of 0.04 M. Negative differential resistance has been reported elsewhere in memory devices.[20]

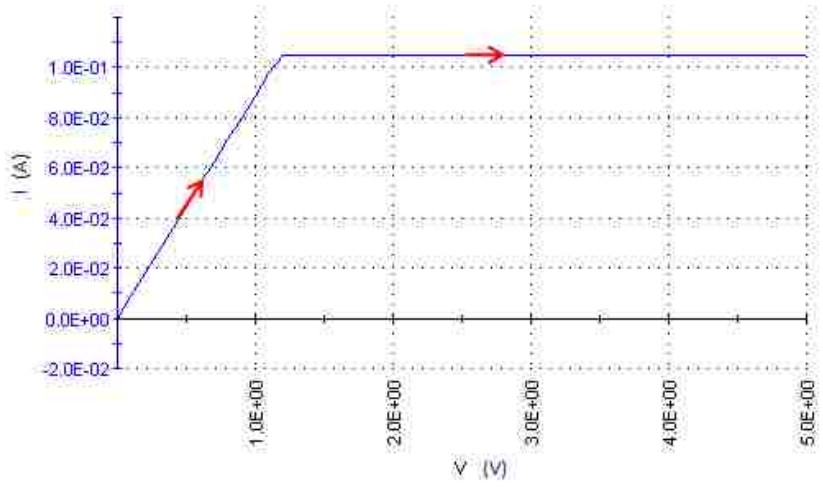

Figure 3.5. Voltage scan (PANI/Au nanocomposite memory device on a precleaned glass slide with an Au sputter coating: initial $HAuCl_4$ concentration of 0.05 M) after switching the device to the ON state.

Various devices, which were made from PANI/Au nanocomposites, showed the characteristics of a memory device. However, devices made from *bulk* PANI/Au samples

did not exhibit such behavior. For the devices made from PANI/Au nanocomposites, the magnitude of the differences in the ON state current and the OFF state current varied from around 500 to 5000 and the transition voltage varied between 2 to 3.5 V. Figure 3.7 shows a graph representing device characteristics obtained from another device made on a precleaned glass slide with an Au coating on it with an initial $HAuCl_4$ concentration of 0.03 M. Typical average resistance of the device in the OFF state was found to be around 100 k Ω, whereas it was found to be around 150 Ω in the ON state. All of the devices could be used repeatedly under atmospheric conditions.

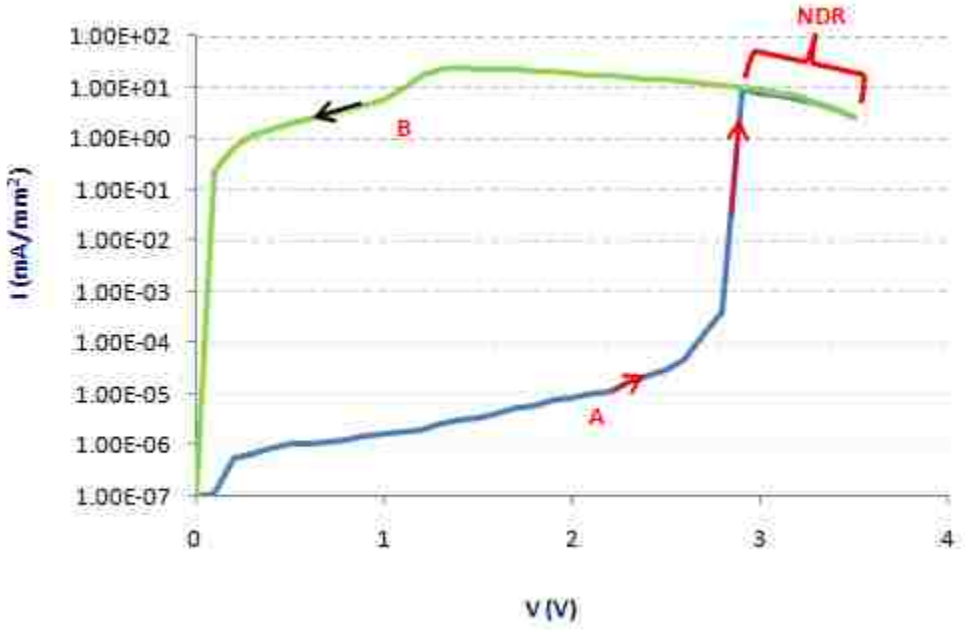

Figure 3.6. Current voltage characteristics of a PANI/Au nanocomposite memory device on a precleaned glass slide with an Au sputter coating: initial $HAuCl_4$ concentration of 0.04 M exhibiting a negative differential resistance region (NDR) after a transition voltage of around 2.9 V.

The transition that occurs from the OFF state to the ON state has been addressed in literature as an electric field-induced charge transfer between gold nanoparticles and PANI nanofibers.[13,29] When the voltage is increased, the electric field between the electrodes increases, and at a threshold electric field, the electrons on the imine nitrogen group of PANI nanofibers gain enough energy to jump to the gold nanoparticles' valence band leading to charge tunneling during the ON state. This redistribution of charges changes the conductance and, hence, shows a large increase in the current. It has been previously reported in literature that due to strong interactions between the metal nanoparticles and the polymer at the interface, the nanoparticles exhibit a non-metallic behavior due to reduction in the density of states near the Fermi level.[22,30] The voltage at which this charge transfer takes place is called the transition voltage. Thus, use of metallic nanoparticles helps to drastically change the properties of the polymer film due to their property of charge storage.[19,20,22]

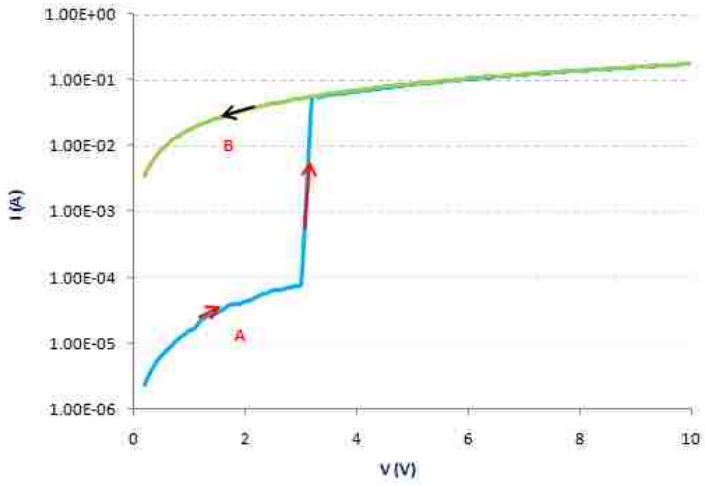

Figure 3.7. Current vs voltage characteristics of a memory device with an initial $HAuCl_4$ concentration of 0.03 M and a transition voltage of around 3.0 V.

3.5. CONCLUSIONS

It can be concluded that by using one-pot synthesis of PANI/Au nanocomposites, it is possible to fabricate a device that has the characteristics of a memory. Our device can work in normal atmospheric conditions and does not need special conditions like a high vacuum, as required for some other PANI/Au memory devices.[13] Our process, being only one-step, is very easy to implement, as well as being an inexpensive method for producing PANI/Au nanocomposites, as compared to other methods described in literature.[13,14] One-pot synthesis enables us to make devices faster and directly on the required substrate. Thus, our method of fabricating a PANI/Au nanocomposite based memory device including the PANI/Au synthesis, certainly appears to be suitable for future industrial-level mass production.

Our devices have been able to show large magnitudes of difference (as large as 5000) between the OFF state and the ON state current. Also, many of the devices had transition voltages of between 2 to 3.5 V, which is comparable to existing semiconductive memory devices. Future work in this area will include fine tuning of the parameters affecting the characteristics and performance of memory devices so that more reliable and reproducible results can be obtained. Fine tuning of these parameters will enable successful fabrication of memory devices, even on flexible substrates (work in progress) with current vs voltage characteristics suitable for a memory device.

3.6. ACKNOWLEDGEMENT

The authors acknowledge the financial support of the National Science Foundation under grant DMR-0706197 (FDB) and the Missouri University of Science and Technology.

3.7. REFERENCES

[1] A. J. Heeger, *Rev Modern Phys.* **2001**, 73, 681.

[2] J. W. Gardner, P. N. Bartlett, *Sensors Actuators A* **1995**, 51, 57.

[3] G. Yu, J. Gao, J. C. Hummelen, F. Wudl, A. J. Heeger, *Science* **1995**, 270, 1789.

[4] C. J. Brabec, N. S. Sariciftci, J. C. Hummelen, *Adv. Funct. Mater*. **2001**, 11, 15.

[5] N. S. Sariciftci, L. Smilowitz, A. J. Heeger, F. Wudl, *Science* **1992**, 258, 1474.

[6] J. X. Huang, S. Virji, B. H. Weiller, R. B. Kaner, *J. Am. Chem. Soc.* **2003**, 125, 314.

[7] S. Virji, J. X. Huang, R. B. Kaner, B. H. Weiller, *Nano Lett*. **2004**, 4, 491.

[8] D. N. Debarnot, F. P. Epaillard, *Analytica Chimica Acta* **2003**, 475, 1.

[9] D. S. Sutar, N. Padma, D. K. Aswal, S. K. Deshpande, S. K. Gupta, J. V. Yakhmi, *Sensors Actuators B* **2007**, 128, 286.

[10] Z. F. Li, F. D. Blum; M. F. Bertino, C. S. Kim, S. K. Pillalamarri, *Sensors Actuators B* **2008**, 134, 31.

[11] E. Smela, B. R. Mattes, *Synthetic Metals.* **2005**, 151, 43.

[12] C. O. Baker, B. Shedd, P. C. Innis, P. G. Whitten, G. M. Spinks, G. G. Wallace, R. B. Kaner, *Adv. Mat.* **2008**, 20, 155.

[13] R. J. Tseng, J. X. Huang, J. Ouyang, R. B. Kaner, Y. Yang, *Nano Lett*. **2005**, 5 1077.

[14] L. Li, Q. D. Ling, C. Zhu, D. S. H. Chan, E. T. Kang, K. G. Neoha, *J. Elect. Soc*. **2008**, 155, H205.

[15] D. Wei, J. K. Baral, R. Österbacka, A. Ivaska, *J. Mat. Chem*. **2008**, 18, 53.

[16] J. C. Scott, *Science* **2004**, 304, 62.

[17] Y. Chen, D. A. A. Ohlberg, X. Li, D. R. Stewart, R. S. Williams, J. O. Jeppesen, K. A. Nielsen, J. F. Stoddart, D. L. Olynick, E. Anderson, *Appl. Phys. Lett*. **2003**, 82, 1610.

[18] L. P. Ma, J. Liu, Y. Yang, *Appl. Phys. Lett*. **2002**, 80, 2997.

[19] L. P. Ma, S. Pyo, J. Ouyang, Q. F. Xu, Y. Yang, *Appl. Phys. Lett*. **2003**, 82, 1419.

[20] L. D. Bozano, B. W. Kean, V. R. Deline, J. R. Salem, J. C. Scott, *Appl. Phys. Lett*. **2004**, 84, 607.

[21] J. Ouyang, C. W. Chu, C. R. Szmanda, L. P. Ma, Y. Yang, *Nat. Mater*. **2004**, 3, 918.

[22] J. Wu, L. P. Ma, Y. Yang, *Phys. Rev. B* **2004**, 69, 115321.

[23] R. H. Friend, R. W. Gymer, A. B. Holmes, J. H. Burroughes, R. N. Marks, C. Taliani, D. D. C. Bradley, D. A. Dos Santos, J. L. Bre´das, M. Lögdlund, W. R. Salaneck, *Nature* **1999**, 397, 121.

[24] C. D. Müller, A. Falcou, N. Reckefuss, M. Rojahn, V. Wiederhirn, P. Rudati, H. Frohne, O. Nuyken, H. Becher, K. Meerholz, *Nature* **2003**, 421, 829.

[25] L. P. Ma, Y. Yang, *Appl. Phys. Lett*. **2004**, 85, 5084.

[26] H. Sirringhuas, N. Tessler, R. H. Friend, *Science* **1998**, 280, 1741.

[27] C. D. Dimitrakopoulos, D. J. Mascaro, *IBM J. Res. Dev*. **2001**, 45, 11.

[28] L. K. Werake, J. G. Story, M. F. Bertino, S. K. Pillalamarri, F. D. Blum, *Nanotech*. **2005**, 16, 2833.

[29] R. J. Tseng, C. O. Baker, B. Shedd, J. X. Huang, R. B. Kaner, J. Ouyang, Y. Yang, *App. Phys. Lett*. **2007**, 90, 053101.

[30] H. G. Boyen, P. Ziemann, U. Wiedwald, V. Ivanova, D. M. Kolb, S. Sakong, A. Gross, A. Romanyuk, M. Buttner, P. Oelhafen, *Nat. Mater*. **2006**, 5, 394.

APPENDIX

TRANSMISSION ELECTRON MICROSCOPE (TEM) IMAGES

TEM images of PANI/Au samples with different initial $HAuCl_4$ concentrations were obtained on a FEI Technai G2 Spirit Transmission Electron Microscope. The precursor solutions were prepared as described in the PANI/Au nanocomposite synthesis in Section 2.2.2. Precursor solutions were coated on a glass slide and exposed to UV for 6 min. They were dried for 4 to 5 hours followed by washing with acetone and DI water to remove the unreacted chemicals. Finally they were dried for 12 hours before they could be used to prepare a copper grid for imaging under the TEM. After drying, a drop of water was put on the dried PANI/Au film. This wet layer was then carefully scratched off from the glass substrate with a non-metallic spatula. The water drop containing dispersed PANI/Au nanostructures was then transferred to a small vial where it was diluted further by adding more DI water. The sample was sonicated for around 3 min. A drop of this PANI/Au nanocomposite dispersion was put on a copper grid containing carbon membrane. It was allowed to dry under vacuum for 12 hours before it was ready for imaging.

Several TEM images for each sample were obtained. From the images for all the samples, it appeared that the nanoparticles size distribution as well as its distribution in the PANI matrix was non-uniform and did not have any specific trend with increase or decrease in the Au concentration in the sample. Hence, it was difficult to make a firm conclusion on the effect of composition on device behavior from the TEM micrographs. However, it was certain from the images that every sample had broad distribution of sizes

of Au nanoparticles and uneven distribution of Au nanoparticles within the PANI matrix. Also, several Au nanoparticles were as large as around 500 nm. Following are some of the transmission electron micrographs obtained from various samples.

Figure A1 is a high resolution image obtained for a sample with initial $HAuCl_4$ concentration of 0.01 M. It can be seen from this image, that the Au nanoparticles are as big as around 300 and 450 nm.

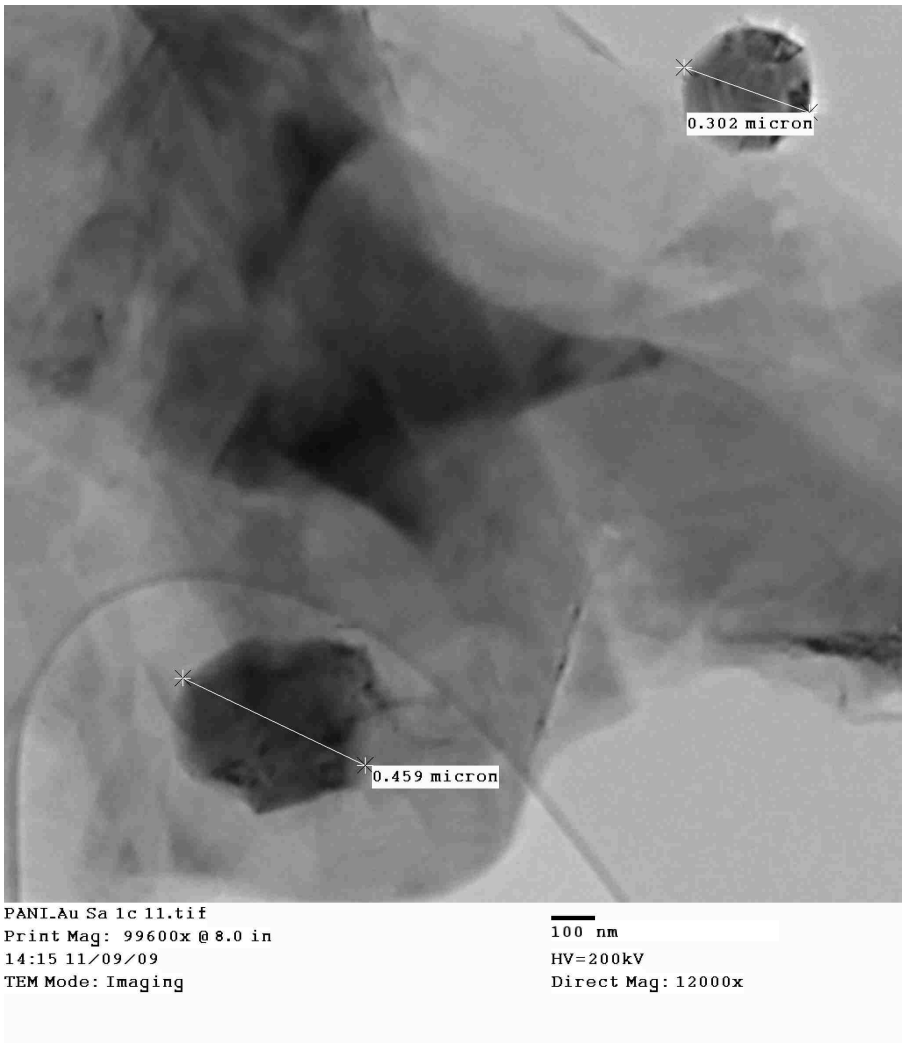

Figure A1. TEM micrograph of a sample with an initial $HAuCl_4$ concentration of 0.01 M.

Figure A2 is also a high resolution image obtained for the sample with initial $HAuCl_4$ concentration of 0.01 M. It can be seen from the image that the Au nanoparticles size is as big as around 450 nm. From Figure A1 and Figure A2, it can be said that some of the Au nanoparticles were very large in size.

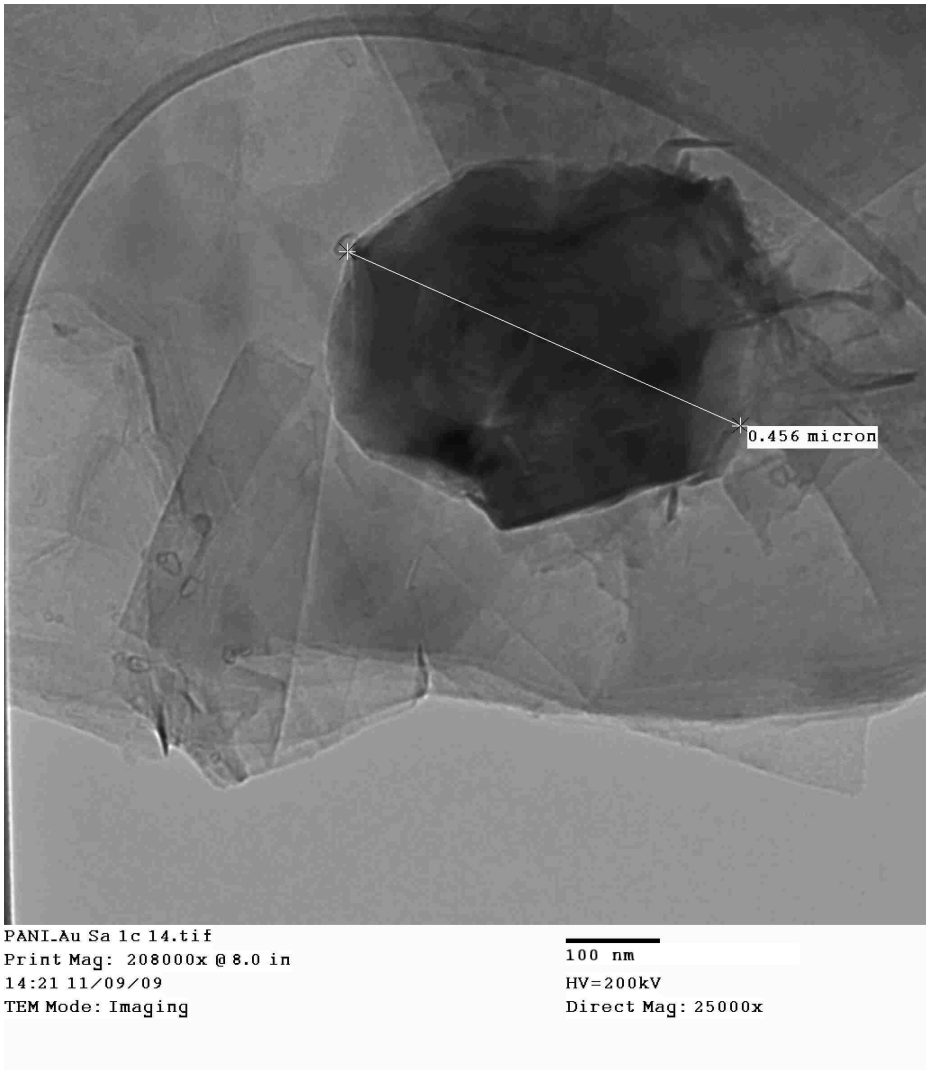

Figure A2. TEM micrograph of a sample with an initial $HAuCl_4$ concentration of 0.01 M.

Figure A3 is a TEM micrograph of a sample with an initial $HAuCl_4$ concentration of 0.02 M. From Figure A3 it can be seen that Au nanoparticle distribution is not uniform in the PANI matrix as well as a large difference in the Au particle size is observed. Some of the particles are around 50 nm and some others being around 500 nm.

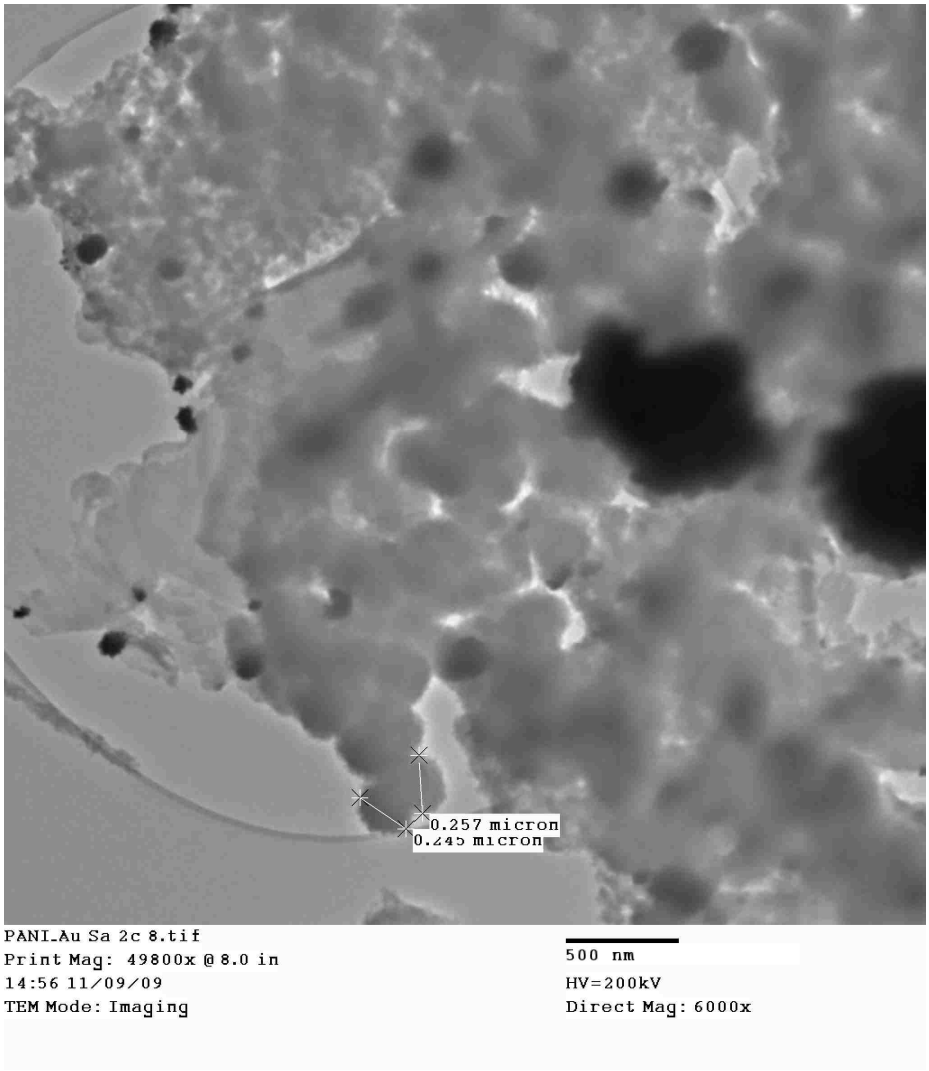

Figure A3. TEM micrograph of a sample with an initial $HAuCl_4$ concentration of 0.02 M.

Figure A4 is a TEM micrograph of a sample with an initial $HAuCl_4$ concentration of 0.03 M. From Figure A4 it can be seen that there is uneven distribution of Au nanoparticles within the PANI matrix and large variation in the size of Au nanoparticles. A good local distribution is observed in some of the regions.

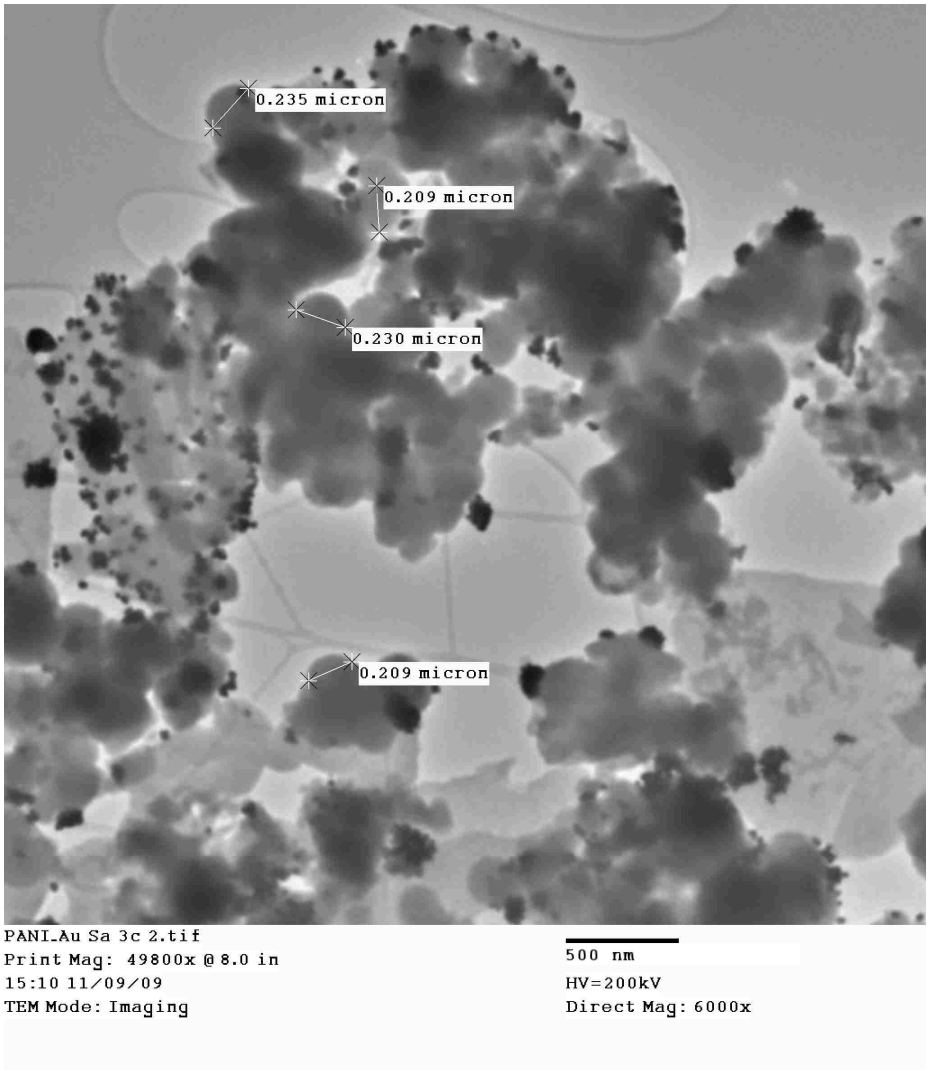

Figure A4. TEM micrograph of a sample with an initial $HAuCl_4$ concentration of 0.03 M.

Figure A5 is also a TEM micrograph of a sample with an initial $HAuCl_4$ concentration of 0.03 M. From Figure A5 it can be seen that Au nanoparticles seem to have a better distribution compared to other TEM images. However, the Au nanoparticles size is as large as 100 to 200 nm.

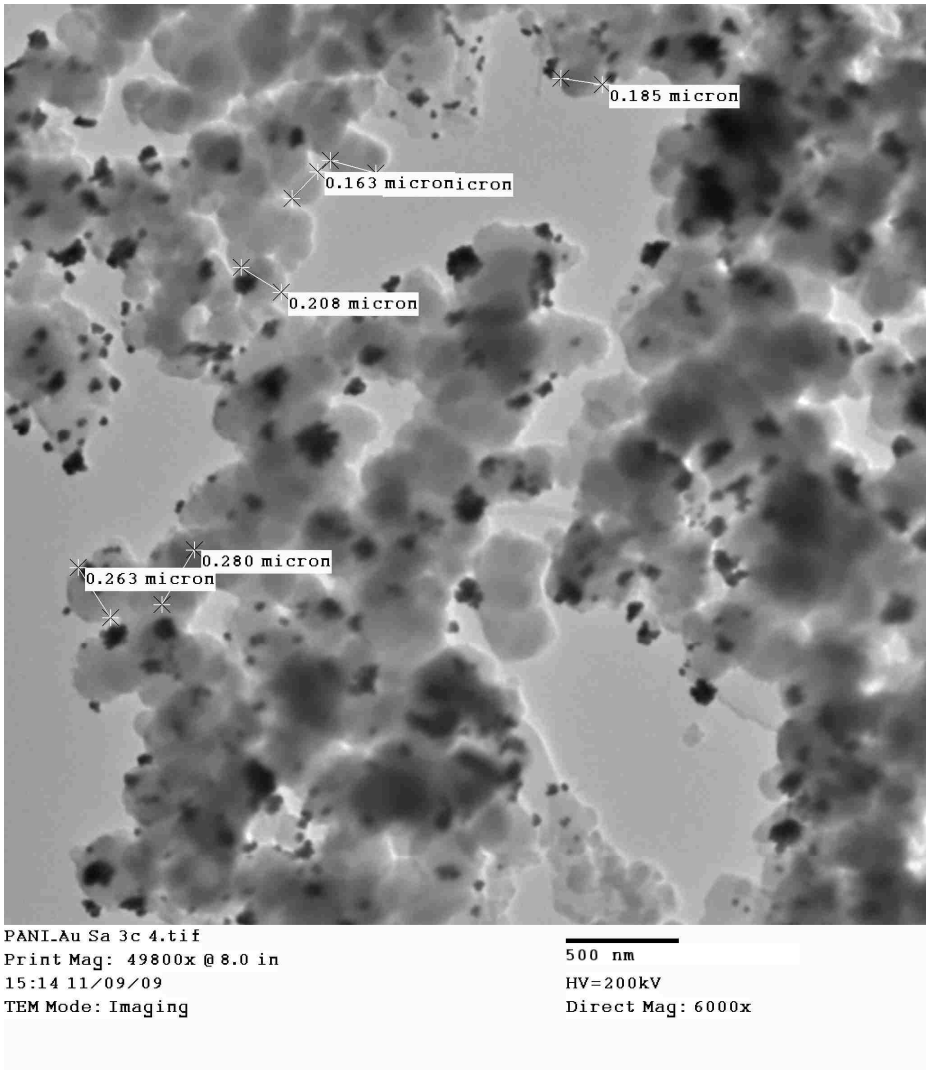

Figure A5. TEM micrograph of a sample with an initial $HAuCl_4$ concentration of 0.03 M.

From all these TEM images, it can be seen that there is a large variation in Au nanoparticles size as well as some of the particles are as large as 500 nm. Also, the Au nanoparticle distribution is uneven in the PANI matrix. It is difficult to comment on the change in Au nanoparticles size distribution, size and its distribution in the PANI matrix with change in intial $HAuCl_4$ concentration. However, such an uneven distribution and large Au nanoparticles size distribution can play an important role in the uncertainty of the device characteristics. Thus, it can also affect the reproducibility of the results.

VITA

Krunal Waghela was born in Mumbai, India on 15th of July 1985. He received his B.E. in Chemical Engineering from Dwarkadas J. Sanghvi College of Engineering affiliated to University of Mumbai, India in July 2007. Krunal Waghela joined Missouri University of Science and Technology in August 2007 to pursue a Master of Science degree in Chemical Engineering. His research was focused on fabrication of memory devices from conductive polyaniline nanofibers and gold nanoparticles.